SMI

CORNELL UNIVERSITY

FLOYD NEWMAN LABORATORY OF NUCLEAR STUDIES

THE CORNELL 300-Mev SYNCHROTRON

D. R. Corson, J. W. DeWire, B. D. McDaniel and R. R. Wilson

(July 1953)

CORNELL UNIVERSITY

FLOYD NEWMAN LABORATORY OF NUCLEAR STUDIES

THE CORNELL 300-Mev SYNCHROTRON

D. R. Corson, J. W. DeWire, B. D. McDaniel and R. R. Wilson

(July 1953)

TABLE OF CONTENTS

(A) Magnet C-section; (A') Oversize C-section providing exit space for beam; (B) and (C) Upper and lower pole pieces; (D) Vacuum chamber, or donut; (E) Gun for injecting electrons into the donut; (F) Magnet coil, upper and lower sections; (G) Supports for coil; (J) Magnetic shunts, or flux bars, across pole gap; (K) Insulating blocks which hold flux bars against poles by means of stainless steel straps; (L) Vacuum pumps; (M) Internal target. The gamma-ray beam is indicated by the three divergent lines originating at (M).

Fig. 1. CUT-AWAY DRAWING OF THE CORNELL UNIVERSITY 300-Mev SYNCHROTRON

I. INTRODUCTION

The Cornell electron synchrotron,[1-3] constructed and operated with the support of the Office of Naval Research, has been producing experimentally useful beams for nearly four years and has been operating at full energy for over three years. Gamma-ray intensities of about 10^{10} "equivalent quanta" per minute can be obtained.

Acceleration takes place in a donut-shaped glass vacuum chamber which rests in the gap of a toroidal electromagnet consisting of 24 C-shaped sections with open faces toward the center of the magnet. The magnet coil is wound through the windows of the C's, above and below the orbital plane. The magnet is tuned to resonance at 30 cycles per second with a large bank of capacitors. In normal operation the peak flux density in the magnet gap is 10,600 gauss, corresponding to an electron energy of 318 Mev at the design orbit radius of one meter.

Electrons are injected into the donut with energies up to 100 Kev with an electron gun. Initial acceleration is by betatron action, with the betatron flux provided by saturating magnetic shunts across the magnet gap. The 47.7 mc radiofrequency synchronous accelerating field is turned on at an electron energy of 6 or 8 Mev as the betatron shunts begin to saturate. The RF resonator comprises a 45° segment of the donut, and is made of fused silica, coated inside and out with laminated electroplated silver or copper. An RF voltage of 3000 volts peak can be developed across a non-conducting gap on the inside of the resonator. Near the peak of the 30 cycle accelerating period the RF voltage can be reduced slowly, allowing electrons to spill out of their orbits and strike the target over an extended period, which is advantageous for counting experiments.

Magnet current is stabilized electronically through control of the generator exciting current. Electron injection time is controlled through circuits which measure the relative amounts of visible light radiated by the electron bunch on successive acceleration cycles and adjust the timing for maximum radiation.

Radiation shielding in the vicinity of the magnet is provided by concrete blocks and lead bricks. Radiation intensities behind the shielding can be maintained at low enough levels so that no health hazards are involved. In normal operation the synchrotron is controlled and experimental equipment is monitored in another building, separated from the accelerator room by 30 feet of earth.

Detailed specifications for various parts of the machine are shown in Table I.

Table I

General Data on Cornell University 300-Mev Synchrotron

Magnet: Toroidal type, composed of C-shaped sections arranged radially around a circular orbit with gaps toward the center. Poles attached to top and bottom legs of each C-section.

Weight, over-all	80 tons
Height, over-all	88 inches
Outside diameter	154 inches
Diameter of electron orbit	2 meters
Vertical gap between pole pieces	$3\frac{1}{8}$ inches
Number of C-sections and pole sets	24
Average weight of C-sections	3600 lbs.
Average weight per pole piece	1100 lbs.
Thickness of steel for "C"s and poles	0.014" (29 gauge)
Number of magnetic shunts (flux bars)	24
Average weight of shunts	100 lbs.
Thickness of steel for shunts	0.005"

Two oversize C-sections extend 17" beyond 154" diameter to provide exits for gamma-ray beams from targets.

Coil:

Height of each of two sections	9 inches
Outside diameter	120 inches
Inside diameter	99 inches
Vertical gap between sections	6 inches
Number of cables in coil	18
Number of turns per cable (10 in each section)	20
Active length of each cable	585 feet
Diameter of cables	0.48"
Strands per cable	61
Diameter of cable strands	0.0438"
Strand insulation	Formvar

Cable insulation: Glass tape, half lapped, clear Glyptal impregnated

Excitation:

Generator: 1000 kva, 2300 v, 3-phase alternator, reconnected to furnish 2300 v, single phase A.C., 30 cycles

Usual operating power   185 kw

Tuning: 3 banks of Pyranol condensers in series with magnet coil. Each outer bank 455 condensers in parallel, rated 3750 v rms, 9.3 μf. Center bank varied with desired magnet excitation; usually 48 condensers rated as above and 352 rated 3380 v rms and 13.9 μf. Condensers connected to bus bars by 5000 v, 14 amp fuses. Racks of 36 or 72 connected to bus bars by switches.

Vacuum chamber (donut): Synchronous resonator is incorporated in donut as a single section.

Material, except resonator	Pyrex glass
Material, resonator	Fused silica
Number of glass sections	21
Arc per glass section	15°

Arc of resonator section 45°

Chamber cross section: Elliptical, 7-1/8" wide x 2-13/16" high

Nominal wall thickness   5/16"

Inner surface, glass sections: Silver plated in 3/8" wide longitudinal
strips

Resonator surface: Silver plated inside and outside in 1/4" wide
longitudinal strips

Chamber evacuated by a CVD-556 Kinney pump backing two MCF-300 D.P.I.
diffusion pumps on opposite sides of chamber.

Injection: Betatron-type electron-gun injector driven by 100-kv transformer.

Cooling:

Magnet: Air cooled by 30,000-cfm blower. Air introduced at base of magnet,
channeled toward gap, exhausted at top. Cooling system permits re-
circulation.

Condensers: Air cooled by 20,000-cfm blower. Air recirculated auto-
matically if temperature drops below 60°F.

II. COMPONENTS

A. Magnet

1. Design

The synchrotron magnet was designed to maintain electrons in a circular orbit at energies up to 300 Mev with a maximum flux density of 10,000 gauss, the corresponding gap radius being one meter. The gap height is 3-1/4 inches and represents a compromise between economic considerations and attainable beam intensity.

The magnet consists of 24 C-shaped laminated-steel sections located radially on an orbit of radius 1 meter, with gaps facing inward (Fig. 2). The pole pieces are built up stepwise in a rough approximation of a wedge in order to allow an uninterrupted circular guide field. The over-all diameter of the magnet is 154 inches; over-all height, 59 inches; total weight, 80 tons. The C-sections are bolted to an annular steel base which is spaced about 1-1/2 feet above the floor to provide access to the center of the magnet from below for cooling and other purposes. Annular metal straps on top of the assembly add to its rigidity. The base is bolted, without shock mounting, to a square concrete pad, 4 feet thick, which floats on the building foundation; there is no rigid connection between the pad and the remainder of the floor in the synchrotron room. The center hole in the base plate and an indentation 2-1/2 feet deep in the concrete pad under the center of the magnet provide a central pit in which vacuum pumps are mounted and into which a man may climb to make installations and repairs.

The C-sections (Fig. 3) are built up of vertical laminations of 0.014-inch silicon steel with loss rating 0.52 watts/lb. for 60-cycle excitation and 10,000 gauss peak field. The steel was obtained from the Wheeling
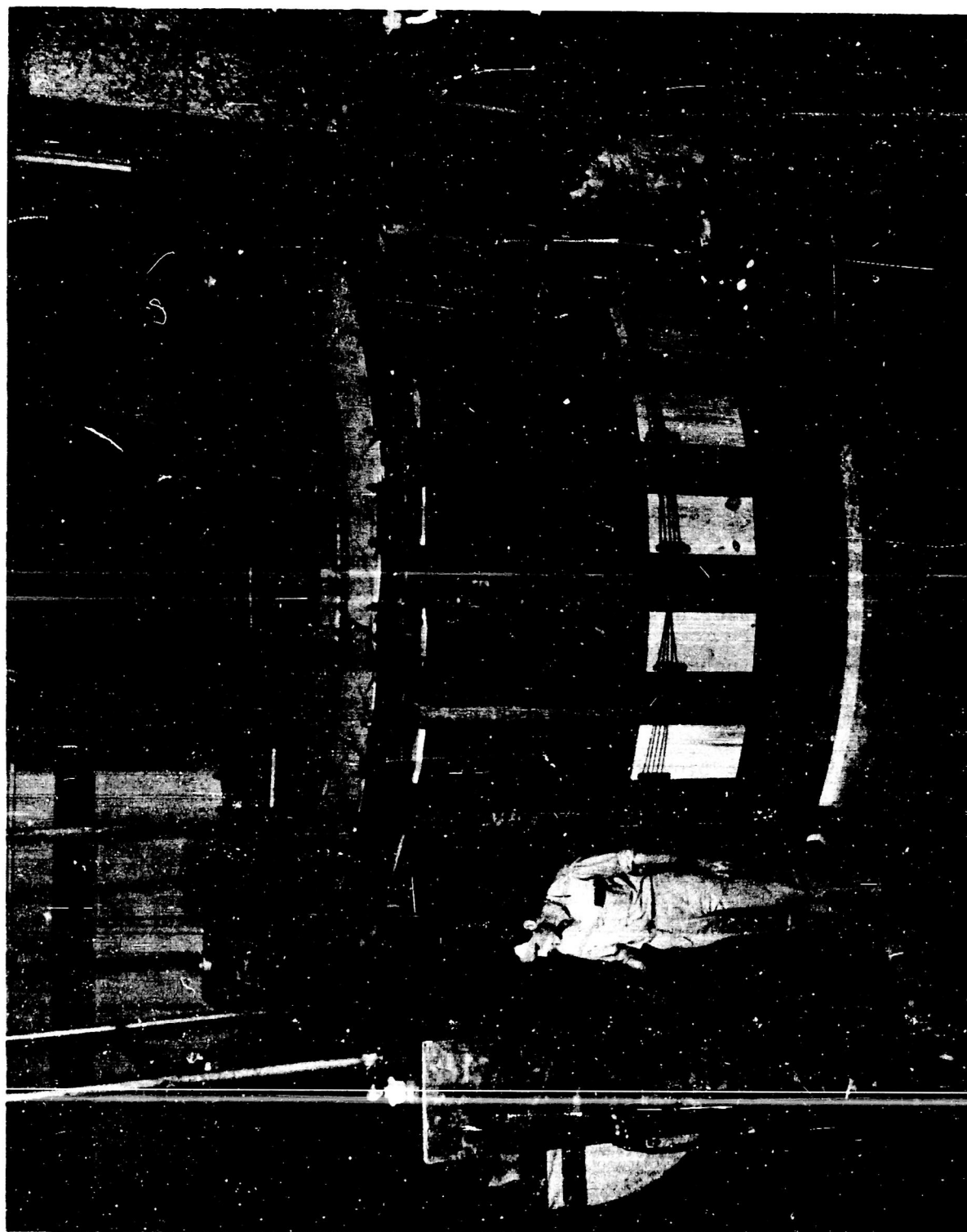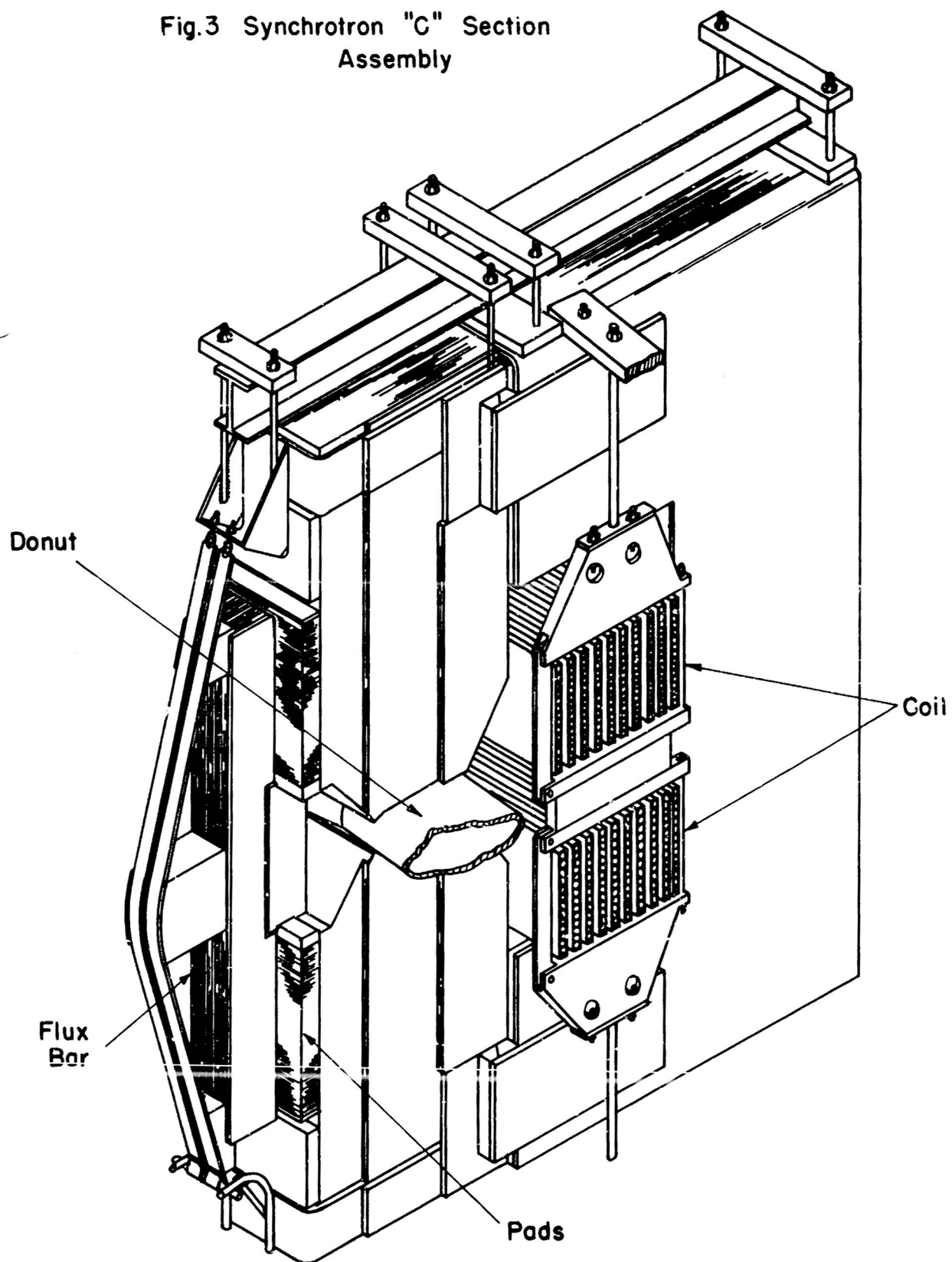
Fig.2 Synchrotron During Assembly

Fig.3 Synchrotron "C" Section
Assembly

Donut

Coil

Flux
Bar

Pads

Steel Corporation[4]. The laminations were cut to proper shape by the Magnetic Metals Company[5]. They were coated with General Electric enamel No. 9576[6] by the General Electric Company; this particular enamel, which has a silicone base, was chosen on the basis of performance in comparative tests of mechanical, thermal, and electrical properties. The laminations were stacked into C-sections at the New York Naval Shipyard[7], where many structural members, including the magnet base, were also fabricated. Two of the C-sections have longer horizontal legs than all the others; this allows their back edges to be displaced about 17 inches radially outward beyond the 154-inch magnet diameter to permit the gamma-ray beams from the two targets within the donut to emerge from the magnet without striking any C-sections.

The pole pieces, i.e. the vertical members of the C-section which form the gap, are also of laminar structure. They were stacked separately from the rest of the C-section and are merely clamped in place for ease of assembly, ease of adjustment of gap height, and to permit installation and removal of donut sections. Since the clamping plates cover the pole pieces for only a fraction of their length, the pole pieces were vacuum-impregnated with Permafil[6] after stacking, to help bond the laminations.

To provide central flux through the donut for the betatron stage of the electron acceleration, small vertically-laminated steel shunts, called flux bars, are placed across the pole pieces, thereby linking the donut. They are held in place by means of metal straps. Flux-bar laminations are of 0.005-inch Armco[8] silicon steel insulated with a coating of Carlite[8]; before stacking, they were varnished and baked by the New York Naval Shipyard[7]. The flux bars provide a flux of up to 20,000 gauss saturating soon after synchronous acceleration begins. Flux bars are separated from pole pieces by horizontally-laminated steel pads which are designed to channel the flux from the pole pieces to the bars

with minimum eddy currents, or flux drainage, in the pole pieces; this serves
to minimize heating loss and magnetic phase shift in the pole pieces due to eddy
currents.

The coil for the magnet (Figs. 1 and 3) is made up of 18 half-inch
cables connected in parallel outside the magnet. These cables are stacked
vertically and are wound helically through 20 turns. The vertical array of
cables in a turn is separated from adjacent turns by wooden spacers 1/2-inch
thick which are impregnated with paraffin. The coil is wound in two equal
sections of 10 turns each above and below the gap; the 18 connections between
cables on either side of the gap are equally spaced around the magnet. The
cables are of stranded copper. Each strand of the cable is coated with
Formvar[6], and the cable itself is wrapped with two layers of glass tape. The
coil was built by the Hyre Electric Company[9].

In assembling the magnet, the coil was mounted on the base before
the C-sections. The pole pieces were clamped to the C-sections after the
latter were installed around the coil; then flux bars were added.

As designed, the magnet can store energy up to 70,000 joules or more
without saturating.

2. Excitation

A diagram of the magnet excitation circuit is given in Fig. 4. The
generator, which is driven by a 3-phase synchronous motor, is a 3-phase delta-
connected alternator reconnected to furnish single-phase current at 2300 v and
30 cycles. At usual magnet excitation (2500 amps r.m.s.), the generator output
is 80 amps; this causes a slight overload in one of the generator windings,
which are rated at 50 amps r.m.s. each. The field excitation for the generator
is supplied from a direct-current motor-generator whose output is controlled
through a motor-driven potentiometer.
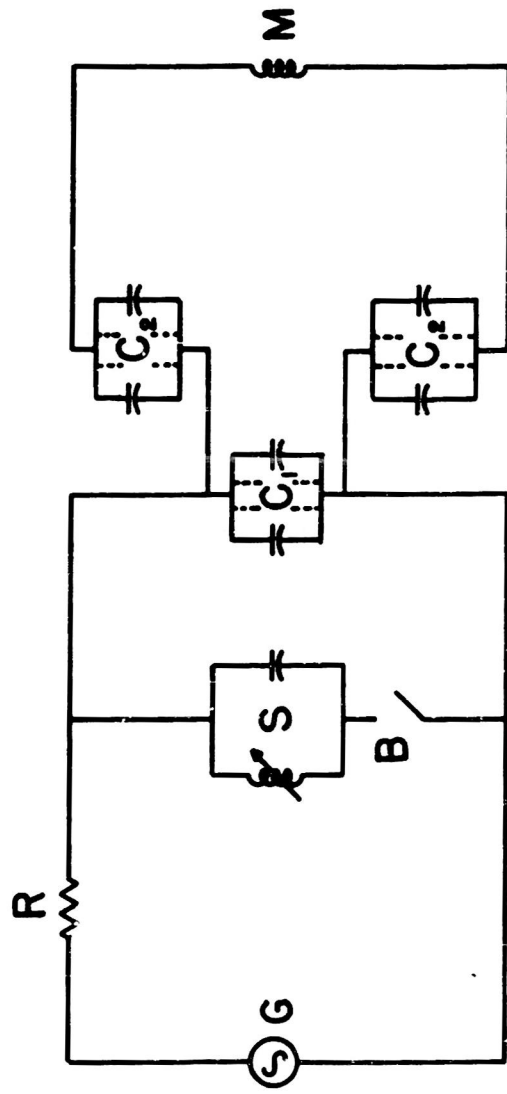
M Magnet

G Generator: 185 KVA At 2300 Volts, 30 Cycles

R Stabilizing Resistor: 0.9 Ohms

S Variable Inductor And Resonant Condenser

B Circuit Breaker

C_1 Center Condenser Bank, Variable

C_2 Outer Condenser Banks

Fig.4 Magnet Excitation Circuit

The resistance R was inserted in the circuit for stability on the basis of initial excitation tests.

Each outer condenser bank C_2 consists of 455 Pyranol [10] condensers rated at 3750 v rms maximum and 9.3 μf for 30-cycle operation. Because the flux bars saturate at a low value of the field in the magnet gap, the inductance of the magnet does not remain constant, but depends on the degree of magnet excitation. At low values of rms magnet current, the inductance is about 40 millihenries, while at usual excitation (2500 amps rms in the magnet), it decreases to about one-third of this value. The center bank of condensers C_1 is always adjusted to allow the generator to run at unity power factor for the desired level of excitation. For usual excitation, the capacity of the center bank is 5,340 μf, making the total of C_1 and C_2 13.8 mf. In preparing to run at lower excitation, condensers in the center bank are disconnected by removing individual fuses, or by opening switches for whole racks of 36 or 72 condensers. Condenser racks and bus bars are of aluminum, with arc-welded joints. Some of the condensers in the center bank have a rating of 3380 v rms and 13.9 μf at 30 cycles, which is somewhat different from the outer bank rating given above.

The dependence of the magnet inductance on the excitation current presents a problem in starting up the magnet. The generator breaker is closed with the generator voltage set near zero; then the excitation is increased to the desired level by increasing the generator field current. With the condenser banks set for resonance at high excitation, the circuit is far off resonance at low excitation during start-up, and the load tends to draw a large leading current from the generator. In order to avoid excessive leading current, which would tend to self-excite as well as overload the generator, the variable inductor S was placed in the circuit. The inductor has an iron core, approximately 15" x 15" in cross section, made up of spare laminations from the synchrotron magnet. The core is wound with two 44-turn coils of 500,000 circular

mil stranded copper wire. The reactance can be varied from about 1 to 17 ohms by moving part of the core along a planer bed with a motor-driven screw. The inductance is at a minimum when the generator breaker is closed, and is automatically increased at a sufficiently fast rate that the generator power factor can easily be kept near unity as the excitation is increased. A small condenser bank is connected across the inductor to tune it to 30-cycle resonance at maximum inductance. The breaker B opens to take the inductor out of the circuit when it has reached maximum inductance. At shut-down, the process is reversed. This device has proved simple and effective for reaching high excitation without drawing excessive leading current from the generator.

Power dissipation in the excitation circuit at 2500 amps magnet current is about 185 kw, of which about 100 kw is dissipated in the magnet, about 60 kw is dissipated as heat in the condensers, and the remainder is dissipated in the stabilizing resistor, generator windings and bus bars.

The characteristics of the magnet excitation circuit are shown in Fig. 5, where the rms magnet and generator voltages and the peak flux density in the gap are plotted against rms magnet current. The flux density was measured by comparing on an oscilloscope the integrated voltage signal from a coil of known area in the gap and the signal from a known voltage source. The non-linearity of the curves in Fig. 5 in the region of low magnet current is due to the presence of flux bars in the magnet. At low currents, when the flux bars are not saturated throughout most of the cycle, the magnet inductance is high, causing steep slopes in the two voltage curves; as the inductance decreases, the slopes decrease. The peak flux density curve would be linear through the origin if the magnet current were truly sinusoidal; however, because of the flux bars, the magnet current is not sinusoidal, but has roughly the shape shown in Fig. 6. The precise shape of the current wave form varies with excitation. The non-linearity of the flux curve results from reading the non-sinusoidal current with an rms ammeter.
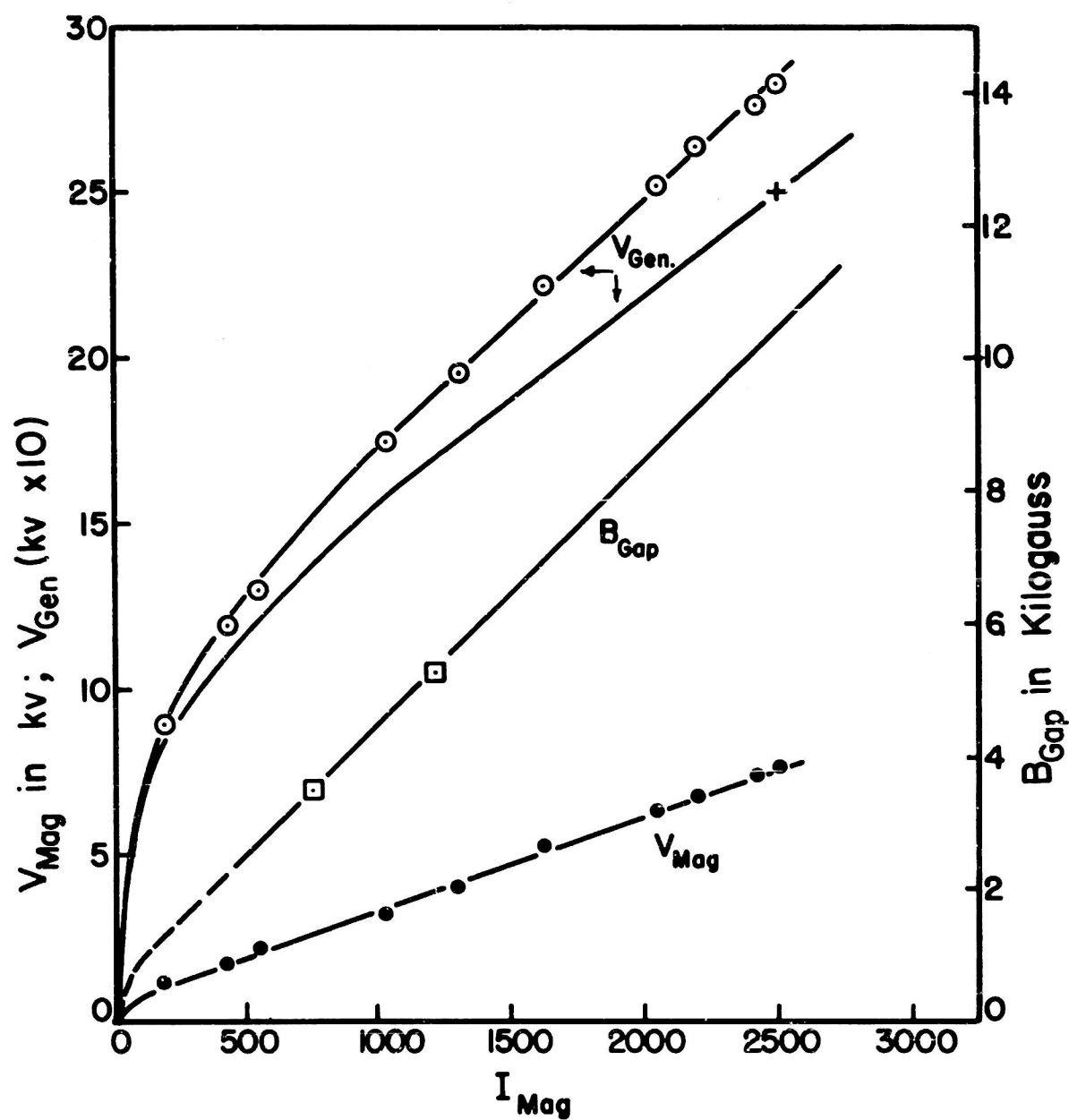
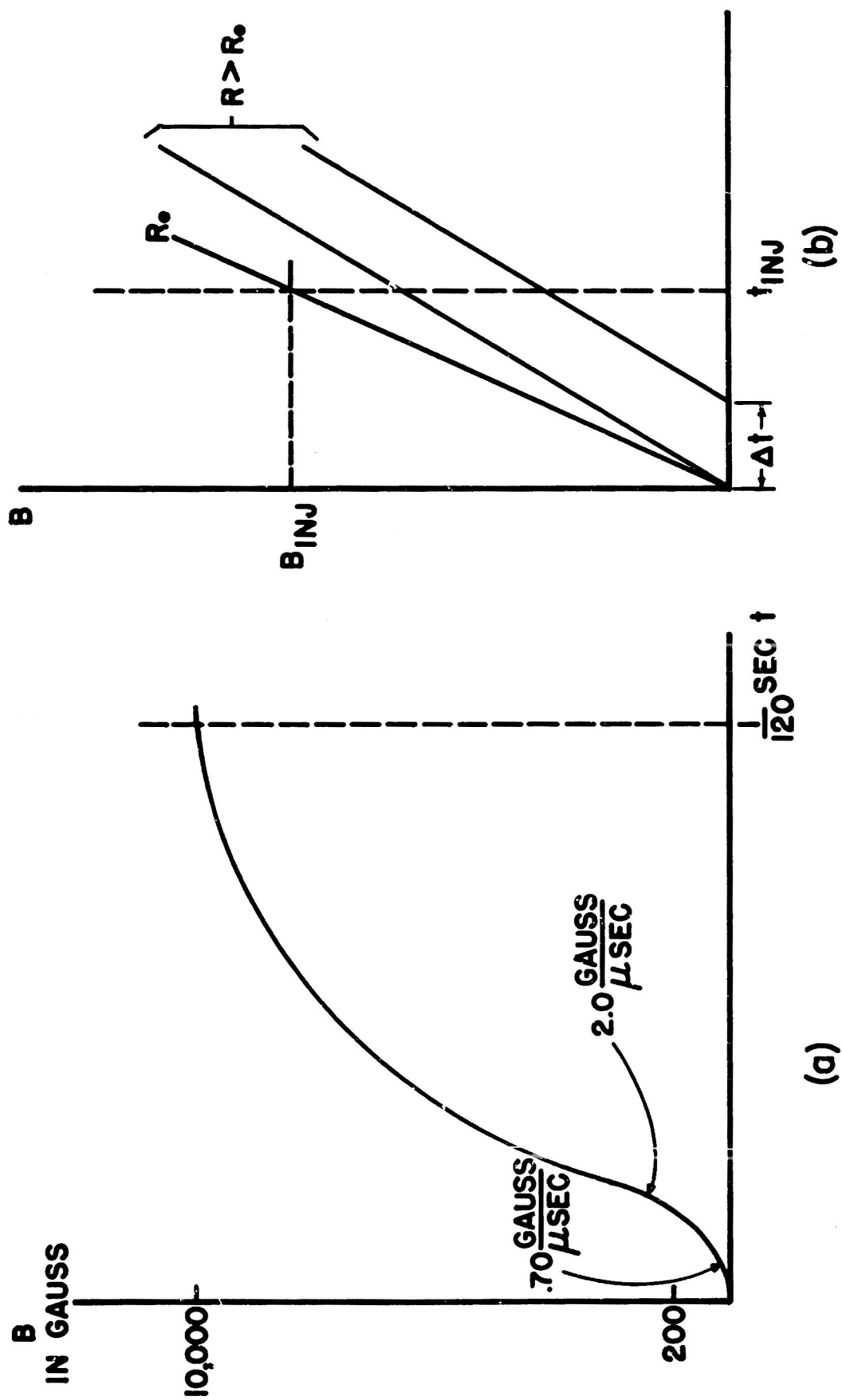Fig. 5 Magnet Excitation Characteristics

Fig. 6 Magnetic Field vs Time

Magnet current tends to fluctuate and drift as various components in the excitation circuit warm up or cool during synchrotron operation. Because a steady excitation level is necessary for consistency of beam energy, an automatic current control system is included in the excitation circuit. A block diagram of the control system is shown in Fig. 7. Magnet current is brought up to the desired value by manual regulation of R_1; then R_2 is set manually to hold the desired current with the Brown amplifier switch closed. If the magnet current varies, the Brown amplifier output pulse will make one of the 6L6 tubes conducting. The direction of the signal to the Brown amplifier depends on whether the magnet current is too large or too small, and determines which of the tubes will be conducting (i.e. during which part of the alternating-current cycle the output pulse will be formed). The amplidyne has two opposed inputs which cause the amplidyne to rotate the motor M_3 in opposite directions, depending upon which tube is conducting. The motor drives R_3 so as to compensate the generator field excitations to oppose the existing variation from the selected magnet current. A motor-driven rheostat was used in preference to an electronic rheostat control because the magnet current takes a long time (a few seconds) to respond to excitation changes and would necessitate the incorporation of huge delays into an electronic control; special delays are not necessary when a slow motor is used. This current-control system holds the rms magnet current to ± 10 amps in 2500, or $\pm 0.4\%$. Its operation is stable in the short run, but there is some drifting in the system which necessitates the resetting of R_2 after several hours of steady operation.

The synchrotron magnet was originally operated at 60 cycles, but was converted to 30 cycles in order to reduce the magnet heating, lower the minimum voltage required in the radiofrequency resonator, and reduce the effects on field perturbation in the gap due to eddy currents.

Excessive heating in the magnet can cause the electron beam intensity

Outer Condenser Bank

Magnet

(80 amp rms)

Inner Condenser Bank

Motor

Motor

(~0.5 amp. D.C.)

Main Generator Field

Field Excitation Generator Field

Aux. D.C.

Outer Condenser Service Bank

(~10 amps D.C.)

R_3

Current Transformer

Motor M_3

(130 V.)   (130 V.)

Magnet Ammeter   **Current Transformer**   **Voltage Rectifier** R_2 **Reg. D.C.**   **Amplidyne**

0-180 V.

Opposed Inputs

A.C.

Brown Amplifier

6L6 Tubes

Shutdown of magnet or
over regulation of R_3 opens
circuit here, automatically
zeroing R_3. Circuit is closed
manually at control panel.
Figures in ( ) for $I_{Mag} = 2500$ Amp.
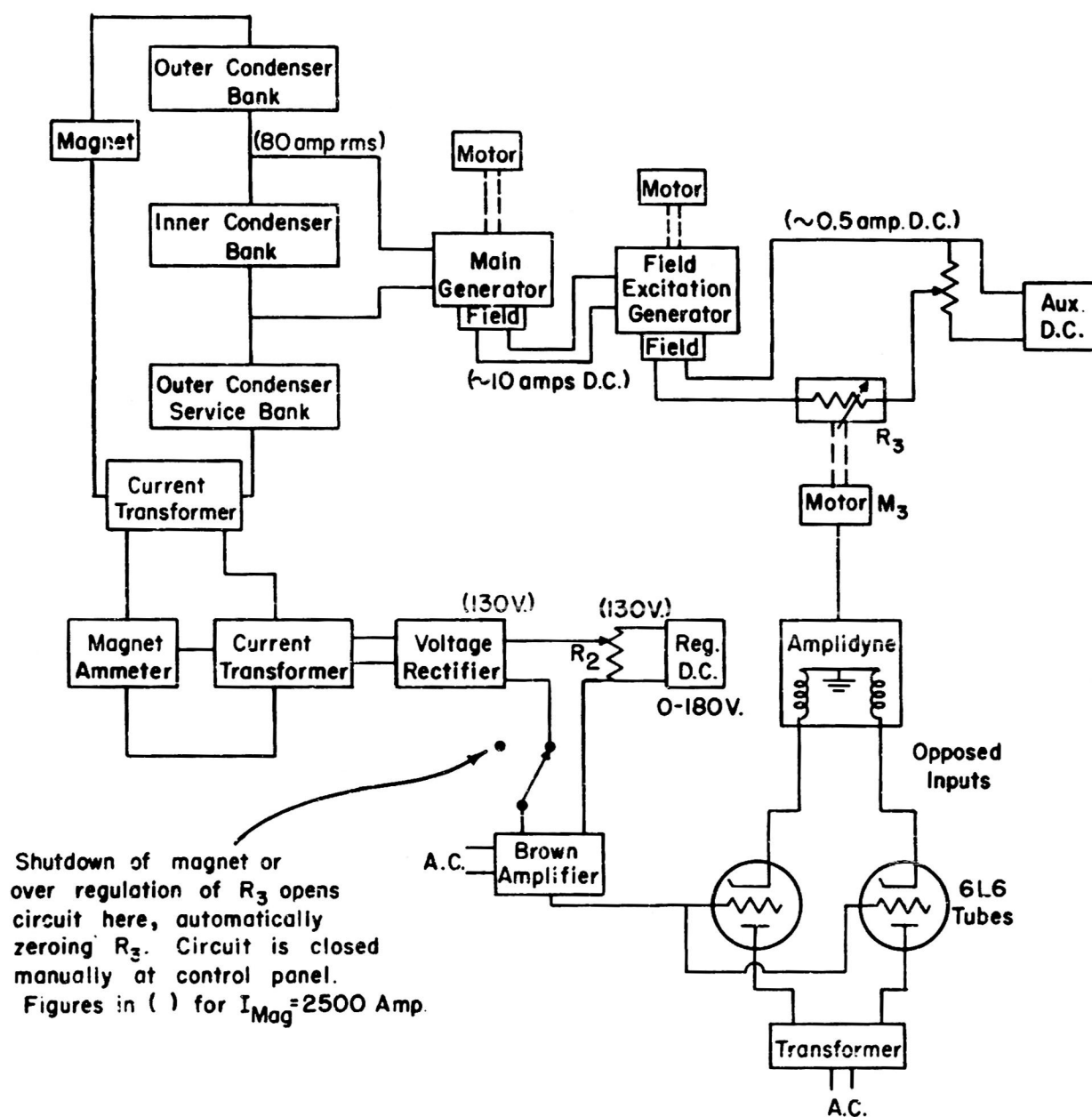
Transformer

A.C.

Fig. 7 Magnet Current-Control System

to drop to low values, or even zero; the reason for this effect is uncertain. Other deleterious effects of overheating are softening of the cement which bonds donut sections, and possibly decomposition of the interlaminar insulation in the magnet. Halving the excitation frequency halved the hysteresis loss; the eddy-current heating loss, which is proportional to the square of the excitation frequency, was reduced to one-fourth by the change.

The minimum radiofrequency voltage required in the resonator section of the donut is determined by the energy to which the electrons are to be accelerated and the time available for acceleration. Halving the excitation frequency doubled the time available for acceleration in each cycle, and therefore halved the minimum voltage required across the resonator gap for acceleration to any given energy. Since it is difficult to maintain large voltages in the resonator, the effect of the change to 30 cycles was to make it easier to attain the maximum acceleration corresponding to peak guide flux density in the magnet gap.

Perturbing fields due to eddy currents are proportional to the excitation frequency; for a given peak field, however, the value of the main field at injection time is independent of the excitation rate. Therefore, when the excitation frequency was halved, the relative perturbing effect on the main field due to eddy currents was reduced proportionally.

The change to lower excitation was justified by the resultant improvement in operation of the synchrotron. The changeover required little rebuilding of components of the excitation circuit: a different generator had to be obtained for 30-cycle operation, several turns had to be added to the coils of the variable inductor, and more capacity had to be added to the magnet and the inductor condenser banks.

3. Cooling

Temperature in the magnet is measured with thermocouples attached to the pole faces, which are the hottest parts of the magnet. Although the insulating varnish is supposed to be stable up to 120°C, the magnet, in the interests of safety, is never operated with the thermocouple reading more than 70°C. No evidence of deterioration of the interlaminar insulation has been found to date.

The magnet is air-cooled by a 30,000-cfm blower which can draw air from outside the building or from a 2-compressor air-conditioning unit. Good beam intensity is obtained when cooling air enters the magnet at about 40°F. At the usual excitation, with about 100 kw of heat loss in the magnet, the air exhausts at about 60°F and the thermocouple reading stays at about 65°C. The outdoor temperature determines how much of the cooling air should be recirculated through the air-conditioner, brought in from outside and refrigerated, or brought in from outside without refrigeration. About 70% of the magnet cooling air is the most that can be recirculated through the compressors.

Cooling air for the magnet is introduced from two ducts at the base and exhausts into a single duct at the top. Airtight canvas panels are connected together by zippers to cover the outside of the magnet between the ducts and force the airflow through the magnet. Canvas and wooden baffles between C-sections and in the center of the magnet channel most of the air through the region around the gap, where heating is most serious.

Since the refrigerating system includes no humidity control, care must be taken not to blow saturated air through the magnet when the magnet is cooler than the cooling air, as it may be at start-up; synchrotrons do not operate well in the rain.

The condenser banks associated with the magnet are located in a locked room which is cooled by a 20,000-cfm air blower. At usual excitation, the heat

dissipated in the condensers is about 60 kw. Cooling air is drawn from outdoors without refrigeration because even on hot days the temperature in the condenser room does not get high enough to cause any damage. However, the blower automatically begins to recirculate the cooling air if the temperature in the condenser room falls below 60°F.

Outdoor air for both blowers is drawn through a single large filter system.

4. Field Measurements

Pole profile

The profile of the magnet pole pieces was designed largely on the basis of a model-testing program. The requirements for the pole pieces, set on the basis of theoretical and economic considerations, were:

1. The field in the gap should vary as $r^{-2/3}$ over a region at least 5 inches wide. (r is the radius from the center of the magnet.)

2. The vertical clearance inside the donut should be 2 inches at the electron orbit, which means that the gap height at the orbit should be 3-1/4 inches at the orbit to accommodate the donut.

3. With a peak field of 10,000 gauss at the orbit, the average flux density in the pole pieces should not exceed 12,000 gauss and no sizable regions of saturation should exist.

4. The profile should consist only of straight lines for ease of fabrication.

The third requirement was satisfied by having the pole pieces beveled from a radial width of 15 inches to 7-3/4 inches at the gap. The bevels make an angle of 35° with the vertical.

Preliminary measurements of field characteristics between pole

pieces were made in an electrolytic bath. The electrodes were double-scale models of the pole-piece profile (15-1/2 inches wide at the gap), and their shape was copied from the pole-piece profile of the University of California synchrotron. Measurements were made with this original shape and with several modified shapes to determine the effect on the field plot of small changes in the profile.

Further measurements were made in the gap of a 1/3-scale direct-current model of the magnet consisting of three adjacent C-sections with pole pieces which were designed on the basis of the preliminary measurements. The iron in this model magnet was machined from boiler plate, except for the pole pieces and flux bars, which were of cold-rolled steel. Field measurements in the gap of the center C-section were referred to the field at a fixed point in the gap of one of the outer C-sections. Measurements were made by a null method using a bridge circuit and two search coils; one coil could be moved in the center plane of the center C-section gap, while the other was fixed at a reference point in an outer gap. Values of relative field could be repeated to 0.1%. The search coils used for most of the plotting were a pair with these features: O.D., 5/32"; I.D., 3/64"; length, 3/8"; winding, 1350 turns of #40 Formex wire; resistance about 45 ohms.

In order to measure the field under conditions simulating the operation of the synchrotron magnet, the model was run through a complete hysteresis cycle and the fluxmeter throw was observed on a rather small change about zero field. A typical cycle consisted of respective current values in amperes of +10, +80, -80, -10, +10; the fluxmeter was observed during the final step.

Because the pole profile does not have cylindrical symmetry, it was necessary to determine the average dependence of the field on r for all azimuthal angles θ from the radial centerline of the center C-section. This was done by taking readings at intervals of $1.5°$, from $\theta = 0$ to $\theta = 7.5$, for each value of r. The average r dependence of the field H was found by numerical integration of

the expression

$$H(r) = \frac{1}{7.5} \int_0^{7.5} H(r,\theta) \, d\theta \tag{1}$$

The results for the three model pole-piece designs are plotted in Fig. 8. The dimensions of the models are given in Fig. 9, together with the final dimensions determined from this testing program.

Flux bar design

Initial acceleration of electrons by the betatron principle requires a rapidly changing flux inside the orbit; to maintain an orbit of constant radius r, the flux ϕ inside the orbit must be related to the flux density B at the orbit by the relation

$$d\phi \simeq 2\pi r^2 \, dB \tag{2}$$

The central flux required for $r = 40"$ is about 5 times the leakage flux from the magnet poles. The necessary flux is provided by placing flux bars of laminated iron in shunt across the magnet gap. The reluctance of the shunt path is adjusted to satisfy the betatron condition, Eq. (2), while the flux bars are unsaturated. As the current in the magnet coil rises, electrons are accelerated by betatron action. As the magnet current becomes large and the flux bars begin to saturate, the central flux becomes smaller than that required for a stable betatron orbit, and the orbit radius begins to shrink; at this time, power is applied to the radiofrequency resonator to continue acceleration by the synchrotron method.

The major conditions to be satisfied in designing the flux bars were the following:

1. The reluctance of the shunt path should satisfy the betatron condition. It was decided to accomplish this by providing for variable air gaps
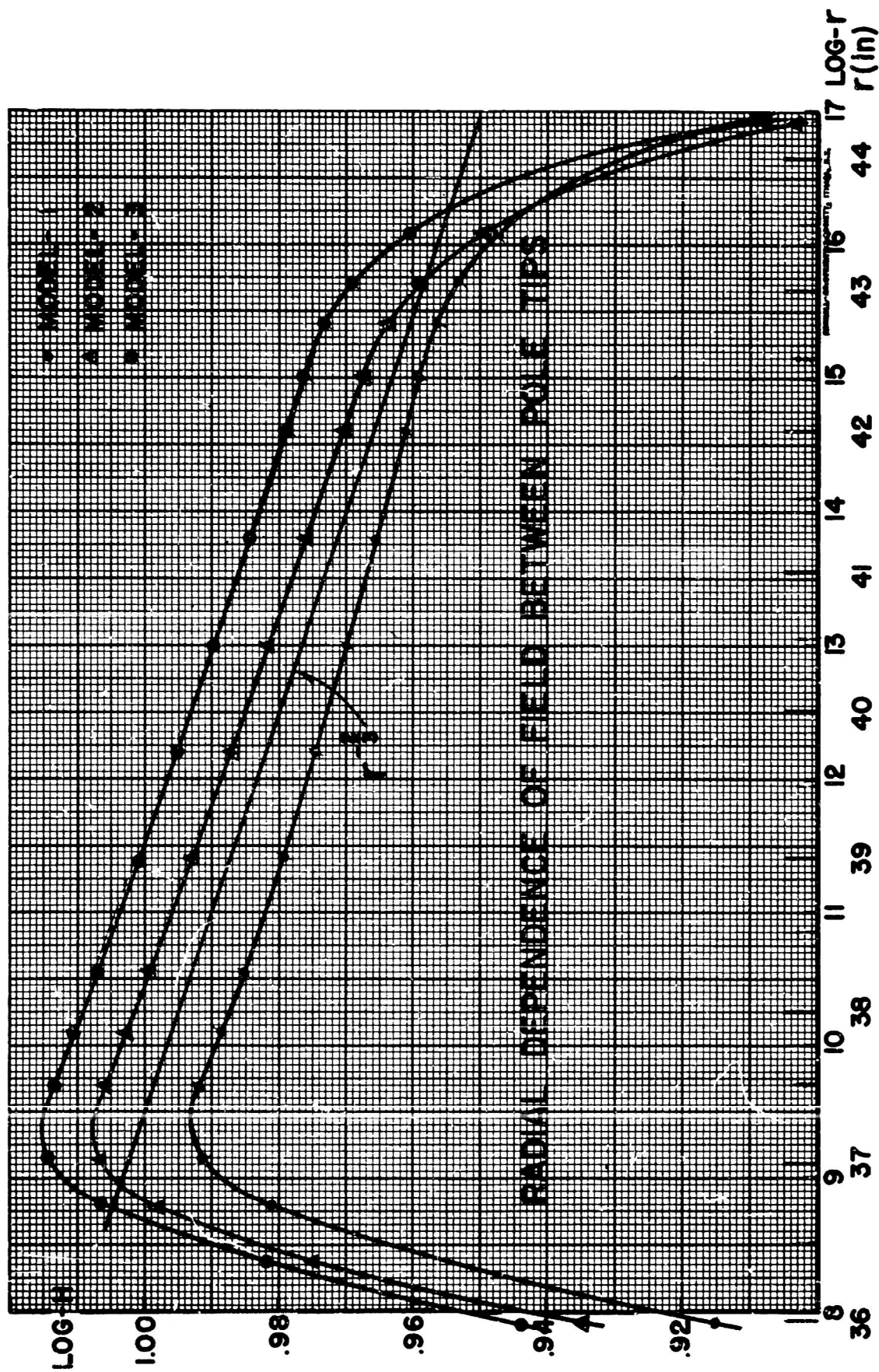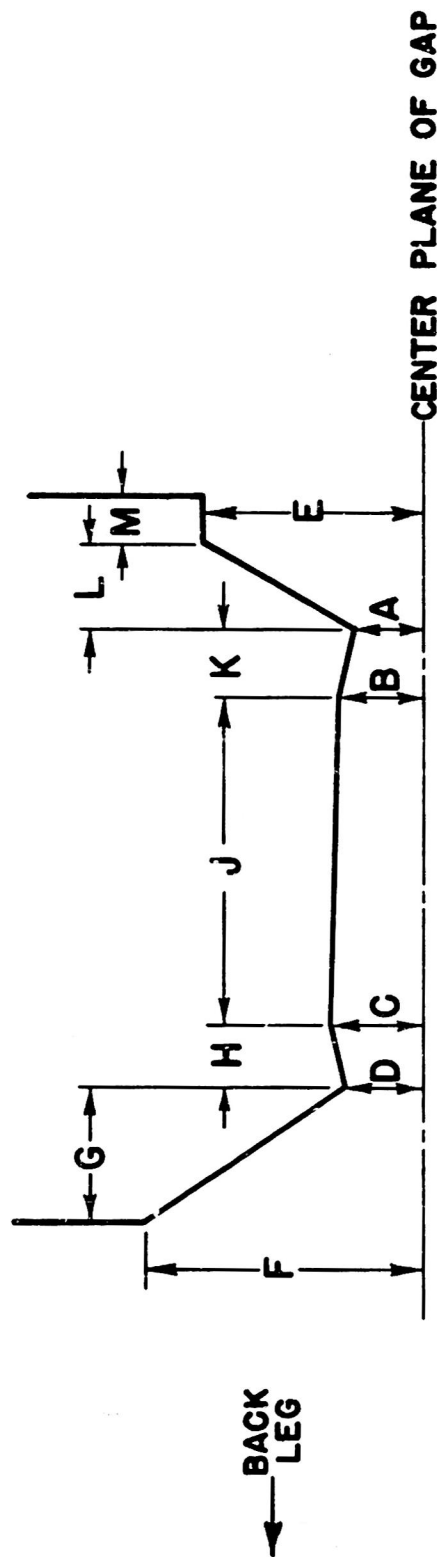
RADIAL DEPENDENCE OF FIELD BETWEEN POLE TIPS

Fig. 8

BACK LEG →

CENTER PLANE OF GAP

DIMENSIONS, VARIOUS POLE MODELS

	TYPE 1	2	3	FINAL SCALE: 1/3	full
A	.4595"	.4605"	.4580"	.461"	1.383"
B	.5165	.5125	.5095	.515	1.545
C	.5665	.5705	.5620	.569	1.707
D	.5195	.5235	.5145	.520	1.560
E	1.790	1.790	1.790	1.790	5.370
F	2.266	2.266	2.266	2.266	6.798
G	1.224	1.221	1.221	1.224	3.672
H	.265	.266	.266	.265	.796
J	1.980	1.980	1.980	1.980	5.940
K	.265	.268	.268	.265	.796
L	.933	.932	.932	.932	2.796
M	.333	.333	.333	.333	1.000

Fig.9

between the flux bars and the C-sections which could be adjusted as required.

2. The flux-bar cross section should be as small as possible. A large cross section is undesirable for several reasons: it makes the magnet gap less accessible; it causes excessive energy storage in the flux bars; it makes excitation more difficult by causing larger generator currents at start-up. However, the cross section must not be so small that the flux bars saturate and the orbit shrinks before the electrons have reached the relativistic velocity required for transition to synchronous acceleration; the instantaneous orbits for betatron and synchrotron action should be the same at the time of transition.

3. The flux bars should be short to minimize energy storage.

4. Flux bars should not perturb the field in the gap; this is most easily accomplished by placing them some distance from the poles.

The behavior of flux in the bars as a function of magnetizing field was studied by means of a small, laminated alternating-current magnet and models of flux bars. The magnet was operated at 60 cycles, which was the frequency then proposed for the synchrotron. The measurements involved the determination of the ratio of the rate of change of magnetic field in the bars to the rate of change of magnetizing field as a function of magnetizing field. Using these measurements, the degree of non-linearity between flux in bars of a given area and field in the gap was calculated for the full-scale machine. The cross-sectional area finally chosen was 11.9 in^2 per C-section, which gave a calculated variation in orbit radius of 0.8"; the magnetic field at the orbit at the time of transition (i.e. when the electrons have been accelerated to 2 Mev) was calculated to be 82 gauss. Later measurements showed the flux bars were actually over-designed, and the cross-section area was reduced to 10.2 in^2. Even with this reduced cross section the flux bars are still over-designed since in actual operation the transition to

synchronous acceleration is not made until the electrons have reached an energy of 6 or 8 Mev.

Heating losses in the flux bars were also investigated. Because the flux in the flux bars changes very rapidly as the magnetic field goes through zero, and because eddy losses are proportional to the mean square value of the rate of change of flux density, there is a considerable heating effect in the bars due to eddy losses. Also, because saturation occurs in the flux bars as the magnet current goes through its maximum, there is severe heating loss due to hysteresis; magnetic flux density is about 21,000 gauss in the flux bars at the peak of the cycle. Eddy losses were calculated from tests on flux bar models using the alternating current magnet described above. Hysteresis losses for various magnet steels were determined from the manufacturers' performance data. The type of steel and thickness of laminations in the final design were determined after considering available cooling capacity, allowable temperature rise, and cost. For operation at 60 cycles, it was estimated that losses in the flux bars would be approximately 0.2 watt/lb. due to eddy currents and 3.5 watts/lb. due to hysteresis.

To provide maximum access to the magnet gap, the flux bars were shaped to cover only part of the face of the inside edge of the pole piece; to further conserve space, the bars were located off center on the pole faces— alternately close together and far apart on adjacent C-sections. In order to minimize flux drainage across laminations in the pole pieces due to these two design features of the flux bars, pads of laminations were included between the ends of each flux bar and the pole pieces which it bridged. Each pad consists of laminations in the horizontal plane, stacked 12 inches high, 1-1/2 inches wide radially, and extending across the exposed face of the pole piece; it is separated from both the flux bar and the pole piece by air gaps which can be adjusted by paper shims. The function of the pads is to draw flux from the pole pieces in a fairly uniform manner, diminishing local variations in field

strength at the main gap of the magnet.

The length of the flux bars is 38"; on the basis of model testing, this
was considered the shortest length which could be used with the assurance that it
would not perturb the field in the magnet gap.

Betatron condition

The flux bars in the completed full-scale magnet (operating at 60 cycles)
were adjusted to satisfy the betatron condition, Eq. (2), with the help of the
bridge circuit shown in Fig. 10. The pick-up coil was a carefully constructed
flat coil with 30 turns in the form of a 30° sector of an annulus of radial width
3" and mean radius 40" which could be positioned anywhere along the orbit in the
magnet gap. The single turn flux loop was placed in a milled slot in a plywood
annulus in the magnet gap: its radius was that of the desired betatron orbit
($r = 39$-$7/8$ inches). The signals from these coils were fed into the bridge cir-
cuit, and the oscilloscope was used as a balance indicator. An integrated signal
from the flux loop was used to produce the horizontal deflection because it was
desired to study in detail the balance near zero flux. The variable resistance
R_1 was adjusted to show zero vertical deflection of the oscilloscope trace at the
time when the guide flux density was zero; this time was marked by a signal from
the peaking strip. When balance is achieved, the following condition holds:

$$\frac{d\phi/dt}{dB/dt} = \frac{R_2}{R_1} \; (\text{NA}) \tag{3}$$

where N and A are the turns and area, respectively, of the pick-up coil. Eq. (3)
is called the betatron ratio. The paper shims which determine the air gap between
flux bars and pads were adjusted until the betatron condition, Eq. (2), was satis-
fied for $r = 39$-$7/8$ inches. A correction coil, described below, is used for fine
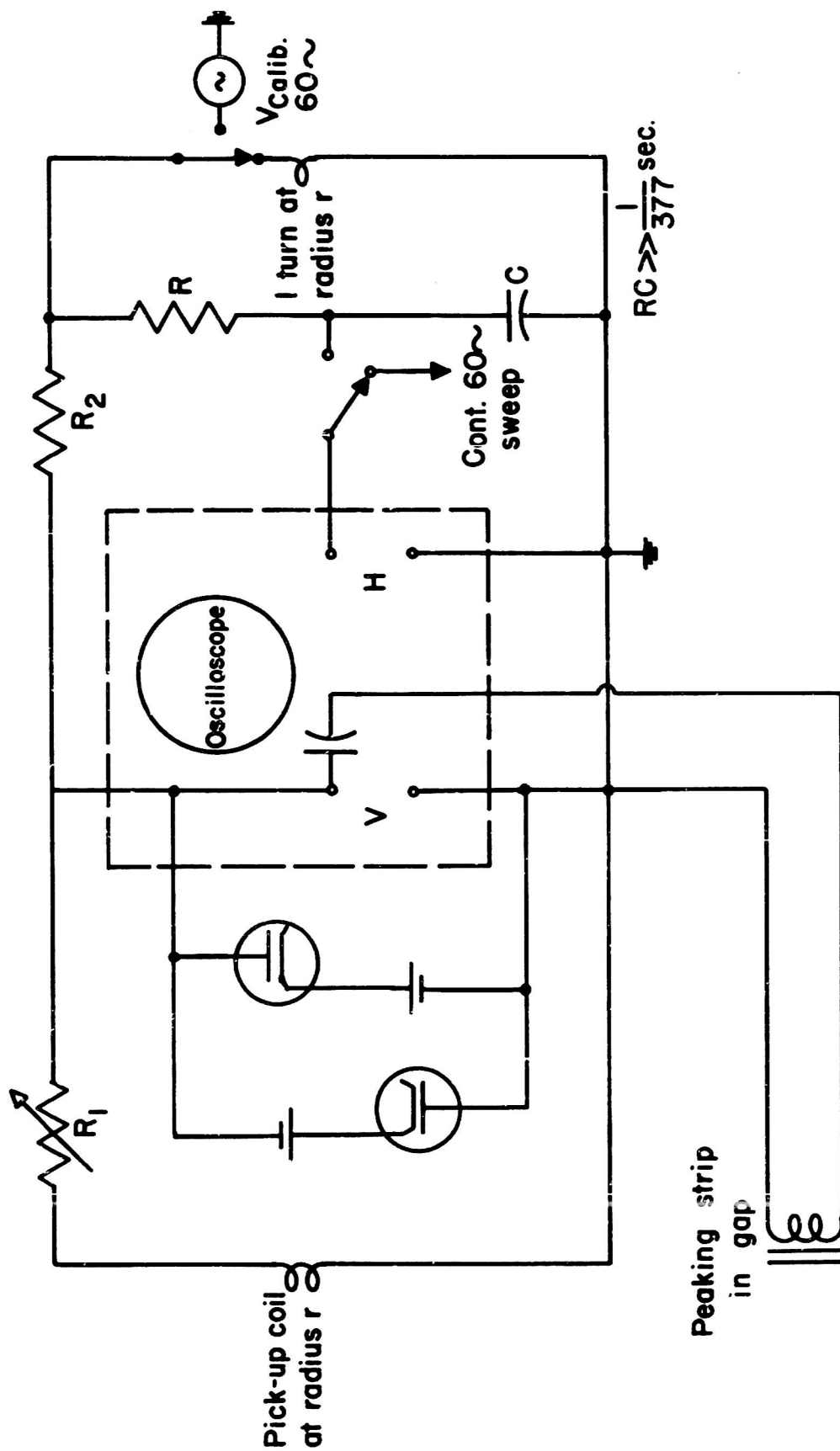adjustments of the betatron ratio.

Fig. 10 Circuit for Magnetic Measurements

The same circuit was used to measure the rate of change of the betatron ratio as the flux bars saturate. Readings were recorded of B_1 for balance at various horizontal distances along the oscilloscope trace. The horizontal scale was calibrated by putting a known 60-cycle voltage through the integrator and comparing curves. Relative decrease of the betatron ratio from the ratio at $B = 0$ was plotted against B up to B = 280 gauss. This plot varied roughly quadratically from 0 to 0.04. The shrinkage of the electron orbit during betatron acceleration due to the decrease in betatron ratio is

$$\frac{\Delta r}{r} = \frac{1}{B} \int_0^B E \, dB , \qquad (4)$$

where E is the relative decrease of the betatron ratio from its unsaturated value. Since the variation of E with B is roughly quadratic, a good approximation to this relation is

$$\frac{\Delta r}{r} = \frac{1}{3} E . \qquad (5)$$

At the transition flux density at the orbit of 82 gauss, E is about 0.004; thus the shift in orbit ratio is only about 0.05", which is much less than the value 0.8" which had been estimated from the flux bar design.

Radial dependence of flux density

Measurements were made in the gap of the completed magnet to see whether the radial dependence of flux density met the condition for a stable orbit:

$$B(r) = B_0 \left(\frac{r_0}{r}\right)^n , \qquad (6)$$

where the subscript designates the stable orbit, and $0 < n < 1$. (Courant[11] gives other limitations on n.) The pole profile was designed to give $n = 2/3$.

Two quantities were measured to check the radial dependence of the flux density: the time derivative of flux density as a function of radius, and the

differences in time at which the flux density goes through zero at different radii. At high densities, small phase differences have no effect; but at low densities, when the electrons are injected, the effect of phase difference can be very great. The influence of phase difference is shown in Fig. 6; (a) gives the variation of flux density with time during a quarter cycle; (b) is an expanded plot of the region near the origin, showing the behavior of the flux density at two different radii, assuming in one case no phase difference and in the other case a phase difference Δt. It can be seen that a phase difference can seriously affect the radial dependence of the flux density. As a first approximation, the effective value of n in Eq. (6) can be expressed

$$n_{eff} = n + \frac{d\beta}{dr} \cdot \frac{dB}{dt} \cdot \frac{r}{B} \quad , \tag{7}$$

where n is the exponent obtained from measuring the time derivative of flux density as a function of radius, $d\beta/dr$ is the phase lag per centimeter increase in radius, and B is the flux density at which n_{eff} is measured.

The relative time derivatives of the flux density at half-inch increments in radius were measured using a circuit similar to that shown in Fig. 10. Voltages from two similar coils, one fixed and one movable, were compared on the bridge. The coils were again 30° sectors of an annulus, but only 1/2 inch wide. Measurements were taken over the entire azimuth, and plots were made for azimuthal increments of 15°. The logarithmic slopes of these plots varied slightly from n — 2/3, but stayed within the limits of zero and one over a region 5-1/2 inches wide.

The relative phase at some 3000 points in the center plane of the gap was measured by comparing the timing on an oscilloscope of signals from a fixed and a movable peaking strip. Readings were taken with the movable strip at five different radii in the gap. The limit of error for each observation of phase difference was 0.1 μsec. Phase difference from the arbitrary fixed

point was plotted as a function of azimuth for each radius; the plots were super-imposed for comparison. It was found that phase does not change with radius near the center of a pole, but that in the region between C-sections there is considerable lag with increasing radius. The effect is caused by flux fringing out of the sides of the poles into the spaces separating them; it becomes more serious at larger radii where the spacing between poles is greater. The fringing flux crosses laminations, inducing eddy currents in them which produce the lagging component.

Relative phases were averaged over azimuth and gave the following results for 60-cycle excitation:

Radius (inches)	Phase lag (μsec)
38-3/8	0
39-3/8	0.11
40-3/8	0.31
41-3/8	0.68
42-3/8	0.99

The phase lag in μsec/cm is seen from these results to be as high as 0.15. Conversion from 60-cycle to 30-cycle operation reduced the lag and also dB/dt by a factor of two. The solution of Eq. (7) for 30-cycle operation, injection of electrons at 100 kev, and acceleration to 300 Mev ($n = 2/3$, $d\beta/dr = 0.075$ μsec/cm, $dB/dt = 0.7 \times 10^6$ gauss/sec, $B = 10.8$ gauss) is $n_{eff} = 1.15$. This indicates that the electron orbit is unstable; but it is closer to stability than with 60-cycle excitation. To bring n_{eff} down to a value between zero and one, correction coils were installed in the magnet gap; these coils are described below.

Azimuthal variation of flux density

Phase differences between poles produce azimuthal flux density variations which can distort the betatron orbit, especially at injection time when the flux density is low and the variations are relatively large. To determine the magnitude of these variations, the measurements of relative phase difference at one radius ($r = 40$-$3/8$ inches) were averaged over each pole and plotted as a function of the pole number (azimuthally ordinal). The plot is given in Fig. 11. This curve was analyzed for its content of the first three harmonics; their amplitudes are indicated by arrows.

Bohm and Foldy[12] have shown that if the flux density is expressed

$$B = B(r) \left[1 + \sum_{f=1}^{\infty} b_f \cos(f\theta + \alpha_f) \right] \quad , \qquad (8)$$

where $B(r)$ is flux density as a function of radius, f is an azimuthal harmonic, θ is azimuth angle, α is a constant, and b is the ratio of harmonic component to $B(r)$, then the oscillations induced by the harmonics will have a relative amplitude

$$\frac{\Delta r}{r} = \sum_{f=1} \frac{b_f}{f^2 + n_{eff} - 1} \cos(f\theta + \alpha_f) \quad , \qquad (9)$$

where n_{eff} is the exponent in Eq. (6). From Eq. (9) it can be seen that the low harmonics of the azimuthal variations are the most serious. Table II gives the solution of Eq. (9) (assuming $n_{eff} = 2/3$) for acceleration of electrons to 300 Mev under two different conditions: the first with 60-cycle excitation and injection at 70 kv; the second with 30-cycle excitation and injection at 100 kv. The results clearly indicate how the relative importance of azimuthal phase shifts decreases when the excitation rate is decreased and the injection voltage is increased. The total amplitude for the first case, which is typical of the early operation of the synchrotron, is of the order of the width of the donut; it necessitated the installation of a series of correction windings, which are
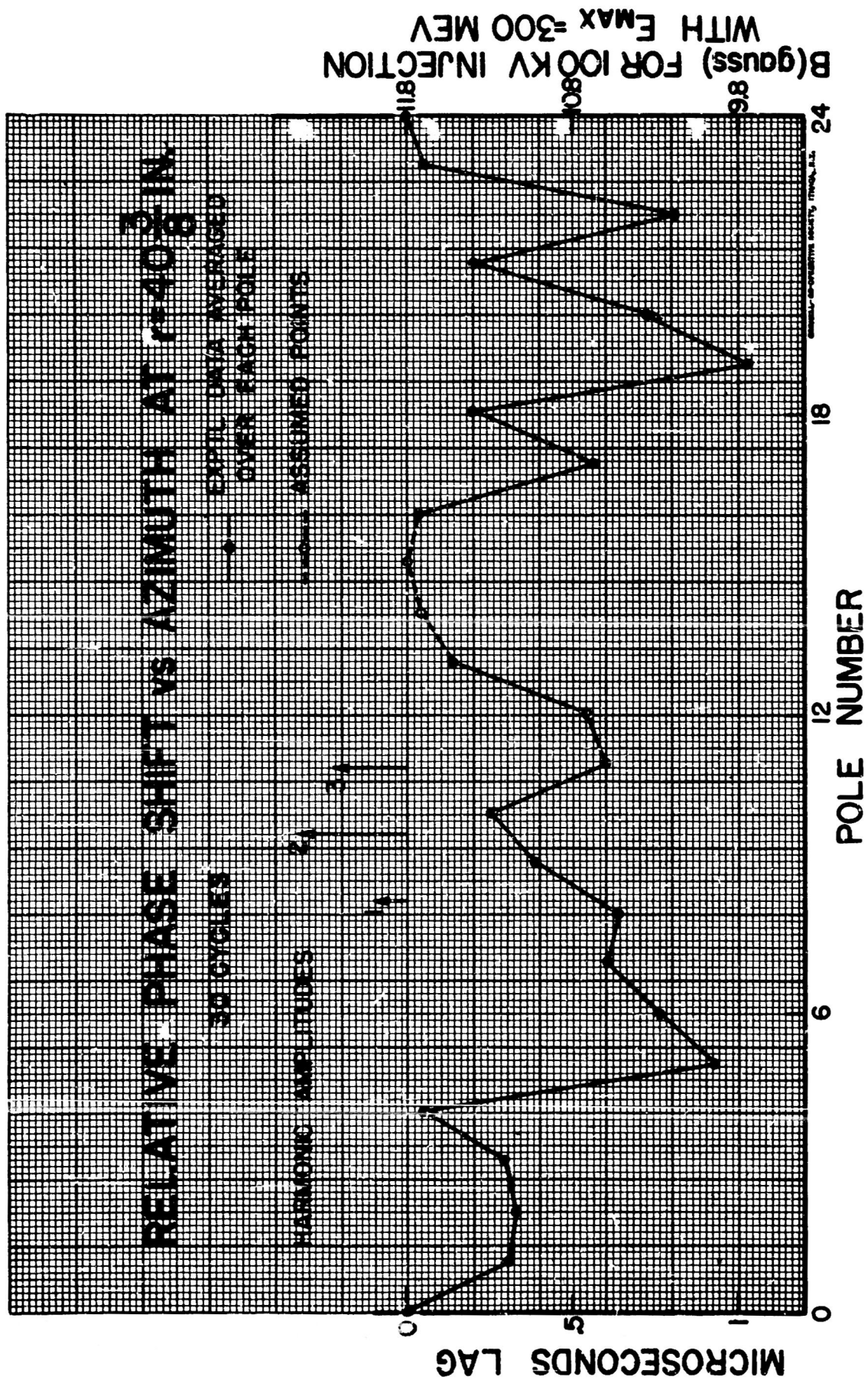
RELATIVE PHASE SHIFT vs AZIMUTH AT $r = 40\frac{3}{8}$ IN.

B(gauss) FOR 100 KV INJECTION WITH $E_{MAX} \cong 300$ MEV

MICROSECONDS LAG

POLE NUMBER

Fig. 11

described below. In the second case, which is more typical of current operation, the total amplitude is only of the order of a centimeter or so; however, the correction coils are still necessary.

Table II

**Effect of Azimuthal Variation of Flux Density on Gap Flux
and on Radial Oscillations at Injection, with Acceleration to 300 Mev**

Azimuthal Harmonic f	60∿, 70-kv injection		30∿, 100-kv injection	
	Rel. Magnitude of Harmonic b_f	Amplitude of Induced Osc. $\Delta r/r$	Rel. Magnitude of Harmonic b_f	Amplitude of Induced Osc. $\Delta r/r$
1	0.034	0.051	0.0065	0.0097
2	0.115	0.030	0.0214	0.0058
3	0.074	0.009	0.0148	0.0017

5. Correction Coils

Radial variation of flux density

The method used for correcting phase shifts in the flux density is indicated schematically in Fig. 12. The radial dependence of the phase is corrected by six single-turn concentric annular coils above the donut and six below. Each coil is insulated and has an annular width of one inch. Corresponding coils above and below the donut are connected in series. A single annular loop and return surrounding the gap flux only drives all of these correction coils through a series of variacs. By adjusting the respective variacs, the individual coils may be excited with either a lagging or a leading phase to correct for the distortion already present. Large variations in setting of the variacs do not have to be made for different excitation levels because the correction remains approximately proportional to the voltage induced in the driving loop. In the latest design provision is made for a differential

Fig.12 Phase Correction Coils
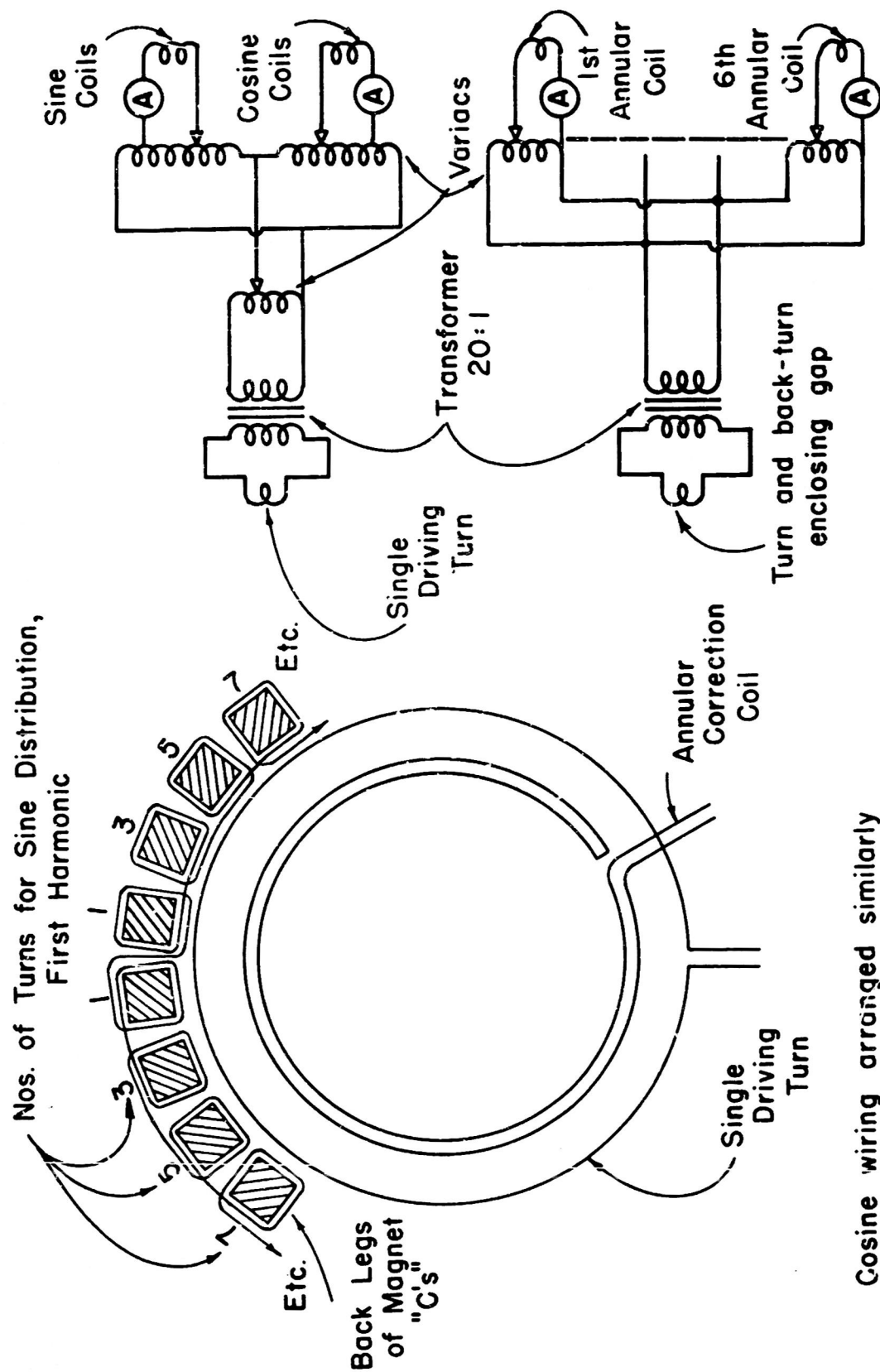
adjustment of the top and bottom coils, to permit raising or lowering the median plane of the magnetic field.

Azimuthal variation of flux density

The azimuthal variations are corrected by six independent sets of windings on the back legs of the C-sections. The number and direction of turns on the C-sections which are associated with these six windings represent sine and cosine configurations for the first three harmonics of the azimuth. Fig. 12 shows the pattern for a winding to correct the first harmonic; if it is to be the sine winding, the cosine winding would be identical in pattern but displaced by 90° in azimuth. All of the windings are driven from a single loop enclosing all the magnet flux through variacs which permit adjustment for the amplitude of each harmonic and the relative amounts of sine and cosine components.

Oversize C-sections

Because of the increased iron path in the two C-sections which extend radially beyond the others to provide a space for emerging gamma-ray beams, these sections lag in phase. The lag is corrected by winding several turns around the back legs of these sections and putting through them enough 30-cycle current in phase with the rest of the excitation circuit to compensate for the lag.

6. Adjustment of Betatron Ratio

The section above on magnet field measurements discusses the betatron ratio measurement and adjustment to satisfy the betatron condition by changing the air path between the flux bars and pole tips. It is both difficult and unnecessary to try to satisfy the betatron condition to better than a few tenths of a percent with this type of adjustment, because a much easier method has been provided.

Fine adjustments in the betatron ratio are made with the magnet in operation. The changing central flux at the beginning of the excitation cycle induces a voltage across the ends of a coil which encompasses all the flux bars. The ends of the coil are connected to drive a variac rated at 750 v and 50 amps. An LR circuit is connected between one end of the variac and its movable centertap in order to provide a variable impedance across the driving coil. Varying the impedance varies the current which flows in the coil. The direction of the current is always such as to reduce the rate of increase of central flux and, therefore, reduce the betatron ratio in the same proportion. By moving the centertap the betatron ratio may be reduced by as much as 1/2%. An rms ammeter is included in the circuit as an adjustment indicator.

7. Performance

The magnet generally operates under conditions for acceleration of electrons to 318 Mev at peak field (315 Mev at the target); this means a peak gap flux density of almost 11,000 gauss. At this level of excitation, the magnet current is 2500 amps rms; power dissipation in the magnet alone, as determined from both electrical measurements and cooling requirements, is about 100 kw. Calculations based on the loss rating of the magnet steel predicted that the magnet power consumption would be only about one-half as large; the excess losses are believed due to eddy currents, but are not understood. The magnet has several times been run successfully at 2700 amps rms for periods of a few hours.

Operating time for the magnet is about 22 hours/day on a good run. Continuous runs extending over a period of days are possible virtually all year round, but on some of the hottest summer days shut-downs of 1/2 or 1 hour in 24 are necessary to prevent overheating. Shut-downs are occasionally necessary because of breakdowns in different parts of the synchrotron; failure of any part of the magnet itself is rare. The most frequent breakdowns are due to vacuum

leaks in the donut and resonator or burned-out injector filaments.

Because of poor accessibility, common repairs take appreciable time.
For example, it requires 8 to 12 hours to remove and replace a section of the
donut. The process involves dismantling the magnet to the extent of removing
several flux bars and lifting a pole piece, as well as removing part of the air
exhaust duct and opening the canvas cover which surrounds the magnet.

Examination of the magnet during periods of shut-down has turned up
some evidence of deterioration. Flapping of laminations on the corners of the
pole tips causes some pieces to break off and fall out, even though wedges are
inserted between pole tips to minimize flapping. Some of these dislodged pieces
of steel have caused short circuiting of the correction coils in the magnet gap,
necessitating the installation of heavier insulation to protect these coils.
Some of the wooden spacers between turns in the magnet coil are being dis-
lodged; but no major damage to the coil has occurred, although two short cir-
cuits have developed. There has been no evidence of any deterioration of the
insulation between magnet laminations. The condensers have offered no special
problems, and show no signs of deterioration.

B. Donut

The acceleration of electrons in the synchrotron occurs in an
evacuated chamber which has the form of a hollow donut and which is placed in
the gap of the magnet. For optimum performance, the properties required of the
donut are:

1. Strength. The donut must not fail or distort when evacuated or when
   subjected to thermal and vibrational stress in the magnet gap.
2. Vacuum tightness. The donut must sustain a good vacuum, must not leak
   or give off gases. This minimizes beam losses by collision.

3. Maximum cross section. For given height and width of the magnet gap, the donut cross section should encompass the maximum area of useful guide field in order to maximize the size of the accelerated beam.

4. Absence of magnetic properties. To avoid distortion of the field in the gap, the donut should be non-magnetic.

5. Charge dissipation. Electron bombardment should not cause charge accumulations on the donut walls which set up unwanted electric fields and distort the beam trajectory. The inside surface of the donut must be conducting, but it must not permit large eddy currents.

The donut presently in use (Fig. 13) is constructed of twenty-one straight Pyrex[13] glass sections, each taking up 15° of donut arc, and one 45° curved resonator section of fused silica. (The resonator is discussed elsewhere in this paper.) The donut cross-section is oval, with outer dimensions 7-1/8 inches wide by 2-13/16 inches high. Wall thickness is nominally 5/16 inches, but this dimension varies by as much as 1/8 inch in the glass sections. The glass sections are all 11-1/2 inches long at the outside edge; their ends are ground flat at an angle of $7\frac{1}{2}^o$ to this edge, so that the sections will each take up 15° of arc when their ends abut.

Fabrication of the glass sections was carried out at the Corning Glass Works, Corning, N.Y. The sections were first blown and cut to approximate size, then ground to proper length and angle on a wet-belt sander. After coating the inside surface with a conducting layer (discussed below), the sections were tempered. They were tested for strength with 45 psi external pressure. Removal of blemishes by end-lapping completed the fabrication.

Not all of the glass sections are simple toroidal sections. Some of the sections have side arms of 2-inch diameter Pyrex pipe protruding at right angles from the inner or outer edge; to these pipes are attached vacuum-pumping tubes,

Fig.13 Resonator and Donut Section

the injector, targets, and detectors. Two sections contain outside ports set at an angle of 30° to the edge to provide exits for the gamma-ray beams from the two targets; these ports are covered with thin lucite windows to minimize the production of secondary electrons in the beam while maintaining vacuum-tightness in the donut.

Joining and vacuum-sealing the donut sections was one of the major problems in the completion of the synchrotron. At present, the glass sections are cemented together in groups of three with Vinylseal Cement type T24-9.[14] Vacuum seals between adjoining groups are made with 1/16-inch molded neoprene gaskets of L-shaped cross-section. One gasket is stretched like a sleeve over the outside edge of each abutting section. These sections are then clamped together in two places by tightening bakelite screw-type clamps hooked over bakelite "ears" attached to the sections. The ears are attached to the outside and inside edges of a section by cementing, lashing with fishline, varnishing the bakelite and fishline with Glyptal[15], and baking.

When the entire donut is installed in the magnet gap, its position can be varied and the pressure at the fluxible joints increased by tightening several bakelite yokes which fit against the donut. These yokes are adjusted by means of threaded bakelite rods which extend from the yokes to the outside edges of the magnet C-sections, passing between the magnet coils.

The donut is evacuated by a Kinney type CVD-556 fore pump[16] and two Distillation Products type VMF-260 diffusion pumps.[17] The vacuum attainable, as measured on an RCA type 1949 ion gage[18] near the diffusion pump, is generally about 10^{-5} mm Hg, and has been as low as 10^{-6} mm Hg.

The conducting inner surface of the donut must prevent charge accumulation and yet be of sufficiently high resistance to keep eddy currents from interfering with the guide field. The synchrotron was originally operated with the donut's inner surface coated with a thin layer of evaporated chromium; this coating did not stand up under the intense electron bombardment near the injector. The

donut sections in present use were painted with silver paint before tempering, then plated with a half-mil layer of silver. The coating is divided into 3/8-inch lengthwise strips by scribing; this keeps the eddy-current effect very small. However, since tests indicate that sufficient charge can accumulate on the scribe lines to destroy the electron beam, the lines are coated with a fairly poor conductor; India ink and various "dugs" have proved satisfactory for this purpose.

C. Radiofrequency System

1. Design requirements

Synchronous acceleration is accomplished by radiofrequency methods similar to those employed in the General Electric Company and Berkeley electron synchrotrons.[19] Accelerating voltage is developed across the open end of a quarter-wave resonator (Fig. 13) so constructed that it forms a section of the vacuum chamber, or donut. A modulated oscillator supplies radiofrequency power to the resonator through a transmission line. The electrical specifications which the system must meet are:

1. **Frequency**. The period of the radiofrequency voltage is just the time of revolution an electron in the gap. For electrons traveling at virtually the speed of light c in an orbit of mean radius $r_o = 1$ meter, the mean frequency f_o is

$$f_o = \frac{c}{2\pi r_o} = 47.7 \text{ Mc.}$$

2. **Voltage**. The energy of an electron traveling at relativistic velocity in an orbit of constant radius is very nearly proportional to the intensity of the magnetic field in which it revolves. A fairly close calculation of the minimum voltage required in the resonator gap can

be made assuming strict proportionality:

The energy of an electron during synchronous acceleration is

$$E \approx 300 \, Br_0 .$$

(10)

For acceleration with a constant orbit radius,

$$\frac{1}{E}\frac{dE}{dt} = \frac{1}{B}\frac{dB}{dt} .$$

(11)

By substitution of Eq. (10) in Eq. (11),

$$\frac{dE}{dt} = \frac{dB}{dt} 300 \, r_0 .$$

(12)

The change in energy per revolution is thus

$$\Delta E/\text{rev} = \frac{2\pi r_0}{c} \, 300 \, r_0 \, \frac{dB}{dt} = 2\pi \times 10^{-4} \frac{dB}{dt} .$$

(13)

The units in these equations are: electron volts for energy; cm. for radius; gauss for flux density; seconds for time. Since the electron energy depends upon the cumulative effect of betatron acceleration, synchronous acceleration, and radiation loss from the orbit, this dependence may be written

$$\frac{dE}{dt} = \frac{dE_\beta}{dt} + \frac{dE_{RF}}{dt} + \frac{dE_{rad}}{dt} .$$

(14)

From Fig. 6, the greatest rate of change of the flux density at the orbit, just after the flux bars saturate, is 2.0×10^6 gauss/sec. Solving Eq. (13), the acceleration of the beam requires that the electrons be supplied 1260 volts/rev for this rate of change of flux density. Measurements show that the betatron action at this point in the cycle contributes 250 ev/rev; there is negligible radiation loss from the electrons, since they are at comparatively low energy and since radiation varies as the fourth power of their energy. Thus, the minimum voltage which must be supplied by the resonator at this time is $1260 - 250 = 1010$ volts. Much later in the cycle the rate of change of the flux density falls far below 2.0×10^6 gauss/sec,

but the radiation effect becomes significant. Maximum resonator voltage is required when the electrons have about 290 Mev, where the rate of rise of the flux density requires 520 ev per revolution and the radiation loss is 655 volts. The betatron action supplies only 95 volts. The resonator, therefore, must supply 520 + 655 – 95 = 1080 ev, or about the same as was required for the steepest part of the flux density curve.

In practice, the resonator must operate at a voltage exceeding the minimum requirement to provide phase focussing. Electrons arriving early at the gap (orbits too small) must receive a higher-than-minimum voltage to be brought into proper phase with the resonator. If the resonator does not supply a sufficiently high voltage, much of the beam may be lost at the time of transition from betatron to synchronous acceleration. Empirically, it has been found that, when the gap voltage is twice the minimum, further increases in the voltage add very little to the beam intensity. Varying the peak voltage produced at the resonator gap varies the time in the resonator cycle at which the electron beam crosses the gap, since the beam tends to "lock in" at the precise voltage required to maintain the electrons in the orbit determined by the resonator frequency.

3. <u>Duration of radiofrequency pulse.</u> It is desirable to have the duration of the radiofrequency pulse variable from a quarter cycle (1/120 sec at 30-cycle magnet excitation) down to some much smaller value, so that the final energy of the synchrotron beam may be set for any desired value over a wide range from the energy corresponding to peak magnetic field to some fraction of this energy. When the radiofrequency pulse is cut off, the beam spirals inward and strikes the target with approximately the energy it had when the pulse was discontinued. Electrons lose energy

by radiation as they spiral and gain some energy by betatron action if the
central flux is still increasing at the time of resonator cut-off; these
two effects determine the time it takes for the electrons to spiral into
the target. The exact energy of the beam at the target depends upon the
magnetic field at the target and the radius at which the target is situated.
For usual target settings, with 2500-amp magnet excitation and full quarter-
cycle acceleration, the electrons reach a maximum energy of 318 Mev at the
design orbit, but drop to 315 Mev by the time they reach the target.

4. <u>Shape of radiofrequency pulse</u>. A pulse modulated by a rectangular gate
will produce a gamma-ray beam from the target which is of short duration,
because all the electrons reach the target within an interval of about 10
μsec. The advantage of such a short electron burst is that its energy
range is small; for peak acceleration, the difference in energy between the
first and last electrons to leave the stable orbit over a period of 10 μsec
is completely negligible, because the guide flux is not changing at the end
of their acceleration. However, a short gamma-ray beam is undesirable for
many kinds of counting experiments because many counts may be missed during
the counter dead time. The gamma-ray beam may be spread out in time by
tapering or shaping the trailing edge of the radiofrequency pulse; as the
peak voltage at the resonator gap decreases, electrons spill out of the
stable orbit over a longer period of time, depending upon the pulse shape.
Electron bursts of the order of milliseconds are obtained by this method,
but at the expense of uniformity of energy. The energy spread is about 2%
in a 1-msec burst with full quarter-cycle acceleration.

5. <u>Starting jitter</u>. Experience indicates that a maximum uncertainty of the
order of microseconds may be tolerated in the on-time of the radiofrequency
pulse.

6. <u>Repetition rate</u>. The maximum frequency of repetition of the radiofrequency pulse is the same as the excitation frequency of the magnet.

7. <u>Eddy currents</u>. Eddy currents in the conducting surfaces of the resonator produce phase shifts in the magnetic field at the electron orbit, and also cause heating of the resonator due to resistive losses. It is desirable to keep these currents at a minimum in order to maintain orbit stability and simplify the cooling problem. Appreciable temperature rise in the resonator complicates the problem of maintaining a vacuum seal at the ends. Eddy currents may be limited by laminating the conducting surfaces using strips about 1/2 cm. wide, and by limiting their thickness to only a few skin depths; for silver, the skin depth is about 0.4 mil.

2. Oscillator

The oscillator which drives the resonator is of standard design, employing a 7C24 tube in a tuned-plate grounded-grid circuit (Fig. 14). The tuning element is a quarter-wave coaxial stub, the resonant frequency of which may be varied from 46 to 49 Mc by adjusting the capacity C. All coupling loops and the length of the cathode feedback line are easily adjustable. The oscillator is modulated by a positive pulse from the shaper which drives the plate. A CW tickler oscillator which is loosely coupled to the main oscillator helps to reduce starting jitter in the main oscillator. Oscillator performance has been reasonably good. It has an over-all efficiency of 50%, and is capable of putting out several times the power required for the resonator. The present design has one disadvantage, however. The frequency and stability of the oscillator are affected by the load, which makes proper tuning somewhat difficult since near resonance the load presented by the resonator changes rapidly with frequency. It would be better to have the frequency-determining element independent of the
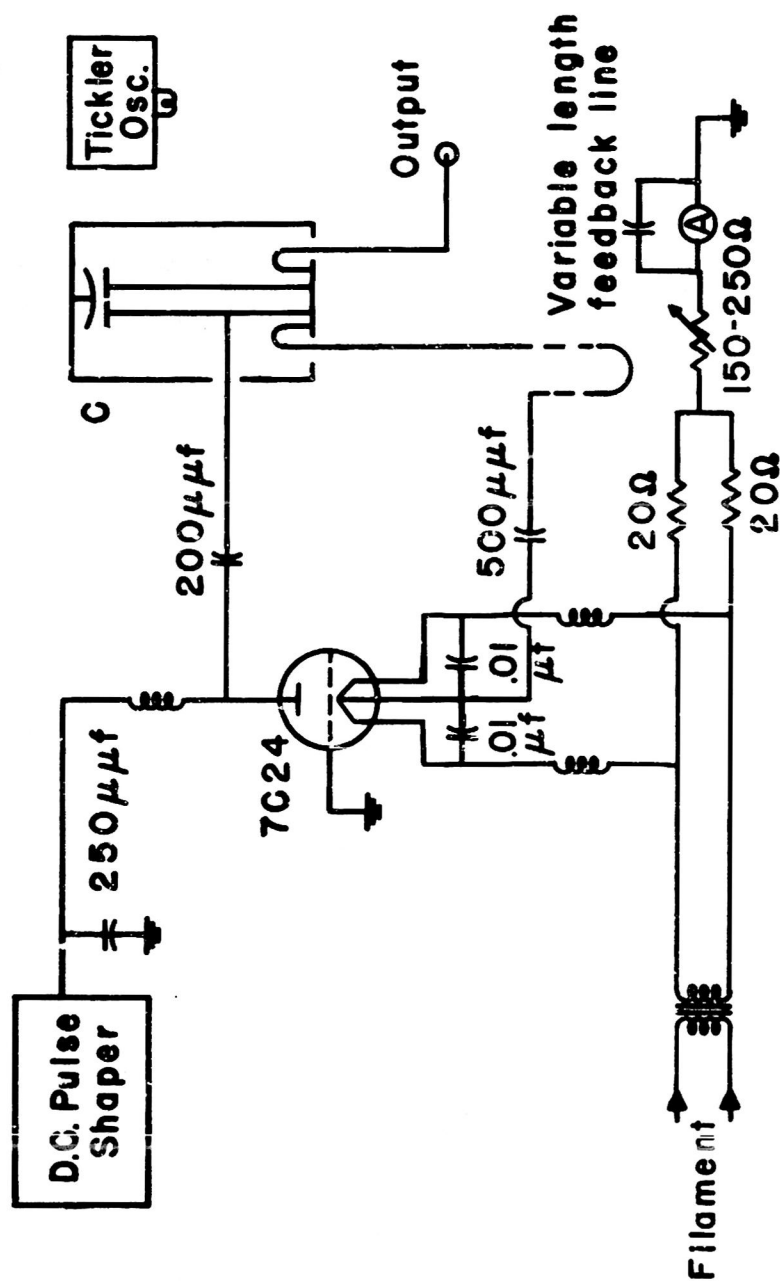
Fig. 14 Oscillator Circuit Diagram

load.

The pulse shaper is designed to give a constant voltage for the first part of its pulse and a decreasing voltage for the remainder; with it, gamma-ray bursts of up to 1 to 2 msec duration can be produced. The length of the pulse from the shaper determines the maximum energy to which electrons in the vacuum chamber will be accelerated; acceleration to 300 Mev requires a pulse 8-1/3 msec long. Timing controls are discussed in a later section of this report.

3. Resonator

The requirements imposed by the operating conditions for the resonator are somewhat contradictory, necessitating delicate compromises among them. Relatively little use could be made of the experience of other synchrotron projects; many construction difficulties were resolved only by trial and error.

As a part of the donut, the resonator's physical shape and cross-section must be in conformity with the other donut sections. The resonator section which was first used was of Corning 707 glass[20], which proved to be unsatisfactory. Since the 45° resonator section could not be blown in one piece, it had to be built up of three shorter sections cemented together; this caused vacuum and other troubles. Furthermore, high dielectric losses in the glass precluded the acceleration of electrons above 100 Mev with 60-cycle excitation. Subsequent resonator sections have been one-piece fused silica sections obtained from the Amersil Corporation[21]. These sections present some problems because of surface irregularities and variable wall thickness, but several resonators have been constructed which permit acceleration above 300 Mev.

The physical length of a quarter-wave resonator is $\lambda/4\sqrt{\epsilon\mu}$, where ϵ and μ are the electromagnetic constants. In the synchrotron, the synchronous vacuum wavelength is just equal to the circumference of the electron orbit. The length of a resonator incorporated into the donut should therefore be

$90°/\sqrt{\epsilon\mu}$; for fused silica, this angle is $48°$. It was desirable to reduce this angle, if possible, to $45°$ for ease of construction and because the remainder of the donut is composed of $15°$ sections. Attempts to lower the frequency of a $45°$ resonator by loading with lumped capacity were unsuccessful. The present tuning method is to reduce the wall thickness by 25% for about 1/3 the length of the resonator from the voltage (gap) end by grinding before the permanent conducting surfaces are added; this lowers the frequency by approximately 8%. Temporary conducting surfaces of copper strips are used in testing. Small adjustments in frequency can be made by varying the location of the gap along the length of the resonator.

The conducting surface of the resonator is plated on after Glyptal[15] scribe lines have been painted and baked on the fused silica to divide the conducting surface into parallel strips. The scribe lines are about 1/4 inch apart, and the conducting strips are about 1/2 cm wide. Silver has been found preferable to copper because it has less tendency to bridge the Glyptal scribe lines during plating. To permit efficient operation of the resonator, the conducting surface should be thick enough to provide a high Q-number. Silver plated to a thickness of 1.1 mils, about three skin depths, affords a theoretical Q of 400, which is very close to the maximum attainable. The thickness is specified as 2 to 3 mils, however, to allow for irregularities in plating. Thicker surfaces are undesirable because they would increase the eddy losses without adding to resonator efficiency. After plating scribe lines are painted with India ink to prevent large charges from accumulating on them due to electron bombardment.

Two methods of scribing are illustrated in Fig. 15. Early resonator models were scribed vertically; they operated satisfactorily in air, but were inefficient when operated between iron poles. Tests showed that the poor performance was due to leakage of the magnetic flux through the scribe lines at the edges of the resonator (Fig. 15a); this flux induced eddy currents in the pole tips. An
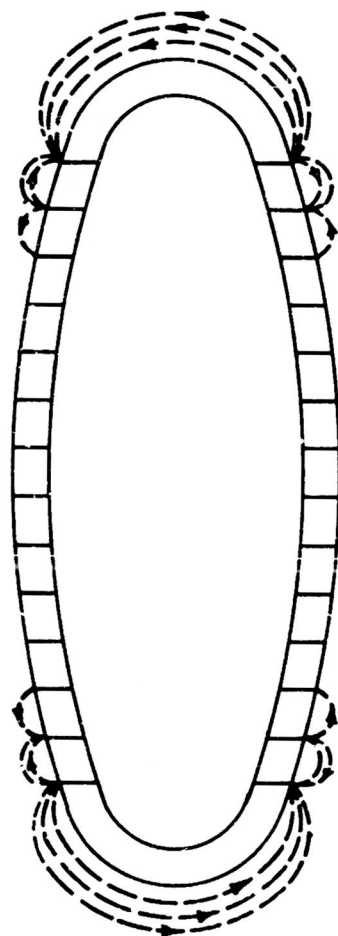
(a)
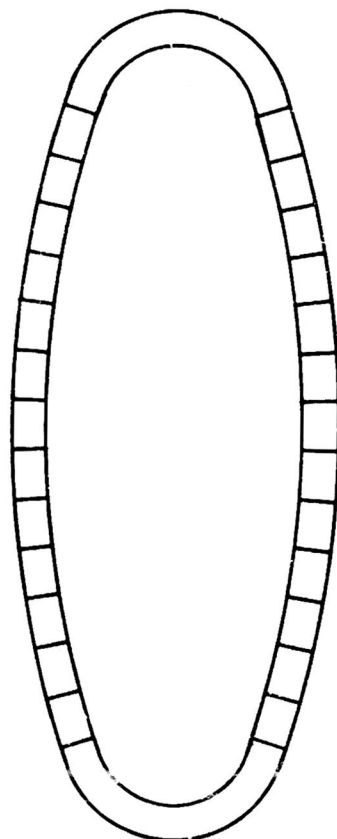
(b)

Fig. 15 Resonator Scribing

50

associated trouble was sparkover between adjacent conducting strips due to a difference in potential caused by flux leakage. More recent resonators have employed radial scribing (Fig. 15b); they operate equally well in air and iron, and give less trouble with sparkover.

Theoretical consideration of the flux leakage with vertical scribing indicates that leakage is to be expected wherever scribe lines on the inside and outside surfaces do not match. Consider a cross section of the resonator wall near the current end (Fig. 16), where inaccurate scribing has caused strips of unequal widths on opposite sides to be connected together. For simplicity, assume that the current in all strips is equal. The total current jw in a given strip is the same on top and bottom, but the current per unit width j varies. The current distribution may be analyzed into two additive components, which are shown with their associated fluxes in Fig. 16 b and c. In b, the current per unit width is equal in all strips; in c, the remainder produces flux leakage; this case may be mapped into the situation shown in Fig. 15a. The voltage associated with a leakage flux may be understood by considering the path abcda in Fig. 17. The path encloses a changing magnetic flux; hence, the line integral

$$\oint \mathbf{E} \cdot d\mathbf{s} = V_{ab} + V_{bc} + V_{cd} + V_{da} = \frac{d\phi}{dt} \tag{15}$$

Since all of the path is embedded in conductor except da, all of the voltages are zero except V_{da}, which must be equal to $d\phi/dt$. This argument is applicable only when ▓ $\ll \lambda/4$, but it can be shown that V_{da} is not zero even if cd $\approx \lambda/4$.

Two silver straps are soldered facing each other around the inside and outside of the resonator to provide additional coupling and to keep all strips at the same potential. Strapping the resonator in the center results in higher efficiency and a slightly higher frequency than strapping at the gap; locating the cross straps at the center also lowers the voltage between strips associated

CURRENT DISTRIBUTION IN RESONATOR WITH NON-UNIFORM STRIPS

(a)

(b)

(c)
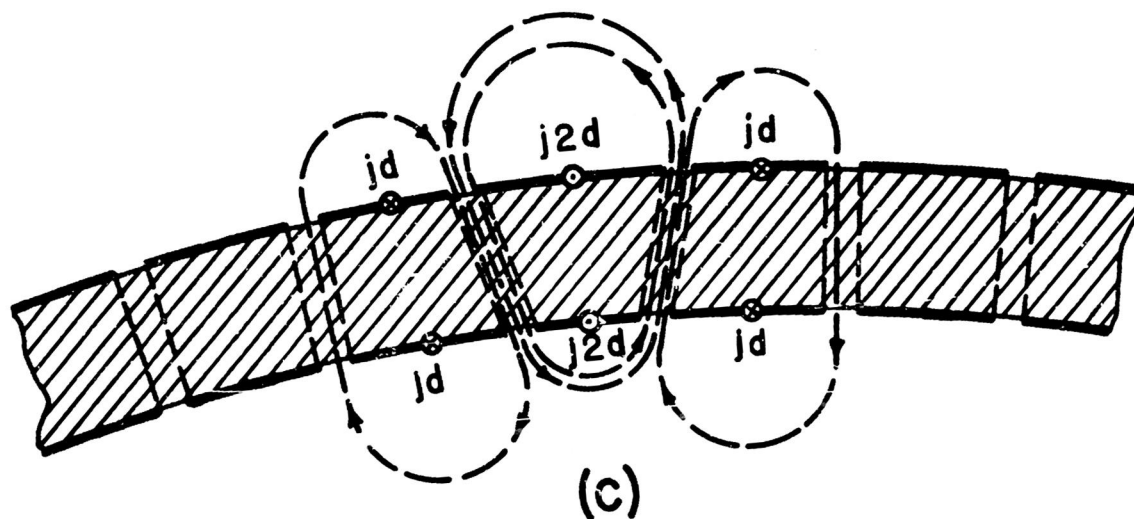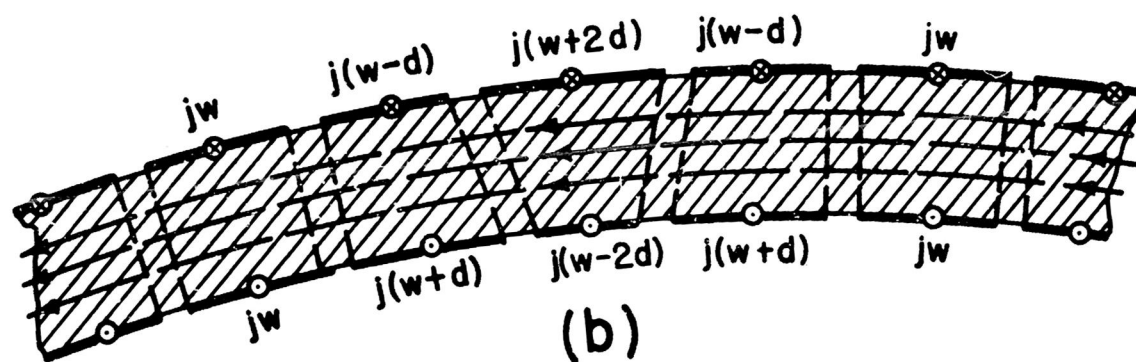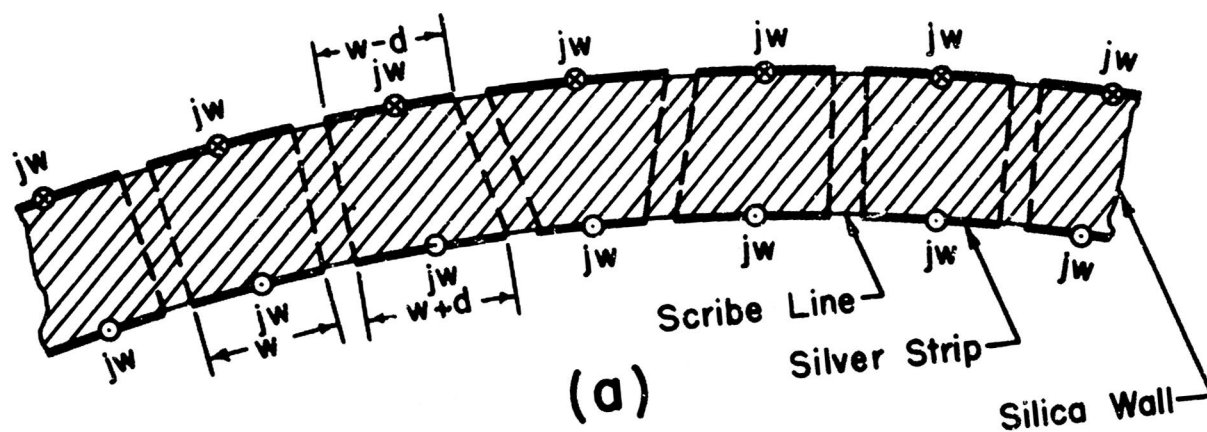
j = average current per unit width of conducting surface
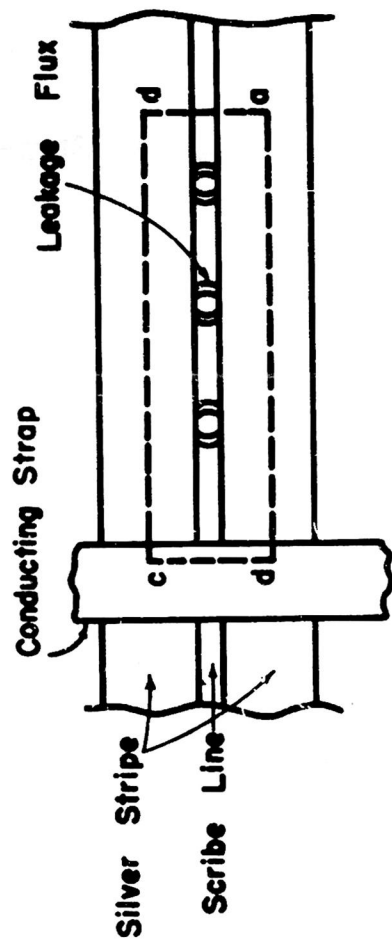w = average strip width

Fig. 16

Fig. 17 Effect of Leakage Flux

with flux leakage through scribe lines.

The driving line from the oscillator to the resonator is a heavy copper wire enclosed in a grounded copper shield. It is connected to the resonator at the inner donut radius. Standing waves in the line may be minimized by connecting it at a point along the resonator where the resonator and line impedances are approximately matched; but the presence of flux bars in the magnet precludes complete freedom to select the drive point. The line has been connected more-or-less successfully in two general ways: by boring a hole in the resonator and connecting the line across corresponding inner and outer strips, or by connecting the line across a break in a single strip. The second method is the simpler, requiring no vacuum seal if the connection is made across an outside strip. The first method is considered preferable, however, because it permits tighter physical coupling and involves less danger of sparkover from the drive strip to adjacent strips. The likelihood of sparkover is further reduced if the line is connected near the current (short-circuited) end of the resonator and away from the voltage (gap) end.

The radiofrequency voltage for synchronous acceleration is developed across a gap cut through the instrips at a position which gives resonance at 47.7 Mc. Gap widths as wide as $5/8"$ and as narrow as $1/4"$ have been used; narrow gaps increase the sparkover problem but reduce the accumulation of charge on the non-conducting gap. The gap sustains potentials of about 2500 volts in air and more than 3000 volts at a pressure of 10^{-5} mm Hg. Installed in the synchrotron, it is normally run at 1700 to 2000 volts. Whether the gap is cut perpendicular to the electron orbit, or is skewed to more nearly equalize the lengths of the conducting strips has no appreciable effect on the performance.

The gap voltage of the resonator is measured by a pick-up meter, in which the voltage induced on an insulated patch on the outside of the resonator is rectified and read on a direct-current meter. This pick-up voltmeter is

calibrated against a standard meter placed across the gap before the final
assembly of the vacuum chamber.

Keeping the ends of the resonator section vacuum-tight has been a
difficult problem. The resonator section is attached to the glass sections by
means of a rubberized sleeve several inches wide which fits over the two adja-
cent sections at the joint. The sleeve is made vacuum-tight over the glass
section by tight binding with fishline; but irregularity of the fused silica
section requires that its end be built up and shaped with cement, or that it be
cemented to the sleeve, in order to maintain a vacuum seal. The cement used on
the resonator section is Insl-x A-150,[22] which combines good mechanical and
electrical properties. Unfortunately, this cement softens at about the resonator
operating temperature and occasionally develops leaks.

4. Resonator tests and performance

Resonators are proved on a test stand before they are used in the
synchrotron vacuum chamber. On the test stand, they are connected by slotted
line to an oscillator of the same design as the oscillator used with the syn-
chrotron. The load impedance of the resonator at the drive point and the power
input are determined from the computed characteristic impedance of the line and
measurements of its standing wave pattern. Power input is measured with the
resonator in air, and also in position between the magnet pole tips.

A well-scribed high-Q resonator should have no "hot" (broken or high-
resistance) strips or flux leaks. "Hot" strips and flux leaks are located with
a small neon bulb, a small pick-up loop connected to a flashlight bulb, or a
small pick-up loop connected to a diode rectifier and ammeter.

Efficiency tests on one of the most recent resonators showed a Q of
550 for an evacuated resonator surrounded by air with 1000 volts peak gap voltage.
The input power was 110 watts. When surrounded by iron to simulate conditions

in the magnet, the Q was 470. In both cases, the resonator was driven at its characteristic frequency of 47.6 Mc.

Vacuum leaks at the resonator have been responsible for a large proportion of synchrotron shutdowns; these leaks are caused by the heating and softening of the sealing cement at the ends of the resonator section. A newly made resonator may last as long as six months without causing a failure; once it begins to overheat, however, renewing the cement seldom keeps it vacuum tight for more than a few weeks at a time unless the cause of overheating is found and corrected or the whole resonator is resurfaced. One resonator failed because of charge build-up on the gap; thickening the conducting strips near the gap so as to shadow it from the electron beam has apparently solved this problem.

D. Injection

Electrons are injected into the donut from an electron gun situated just within the outer edge of the donut. The electron gun is mounted on the end of a long hollow metal stem inside of which are coaxial conductors supplying power to the filament. The stem of the injector passes through a sliding seal into an evacuated side arm of the donut between the two halves of the magnet coil. The radial insertion of the stem and the angle which the focusing slit of the electron gun makes with the vertical can be controlled remotely by a system of gears and two selsyn motors. Stem and electron-gun housing are grounded. Electrons are injected into the donut in bursts by applying high-voltage pulses to the filament through the coaxial cable. Since the electron gun is outside of the stable electron orbit in the donut, the injected electrons spiral inward toward that orbit and do not strike the injector housing as they revolve.

Some of the requirements of a good injector are: vacuum-tightness, large filament output, fairly good focusing, ability to operate stably for long periods, and ability to sustain high voltages. The advantage of a high voltage

at injection is that injection takes place when there is a higher flux density at the gap; orbit distortions due to phase shift effects of eddy currents become relatively smaller with increasing gap flux. The injector design in current use was evolved from the trial of several designs; it has a maximum design output of 100 kv, and is normally operated at about 90 kv.

The injector is fired by pulses from a 10:1 pulse transformer, type NE-304-X,[23] with 100 kv maximum output. The same transformer supplies 60-cycle current to the filament. The pulse rise time is about 5 μsec; it decreases somewhat more slowly. The pulse is originated by discharging a 0.02 μf condenser through the primary, using a 5C22 hydrogen thyratron as the firing switch. The thyratron becomes conducting when it receives a signal from the timing circuit (described in a separate section). The condenser is charged from a variable high-voltage source.

Injection timing must be exact to 0.1 μsec or less in order to maintain a constant beam intensity from successive pulses. Largest electron beams are obtained by timing the high voltage pulse so that it is tangent to the stable orbit electron energy vs. time. The electrons injected at the time of tangency are picked up at the stable orbit and accelerated; those injected at any other time spiral further inward and are lost because they have insufficient energy at injection. The timing circuit can be adjusted to make the two curves tangent for successive pulses, regardless of fluctuations in the injector high voltage supplied to the condenser or of the rate of change of the flux density in the magnet gap. While the timing circuit can be adjusted manually to fire the injector at the proper time, a much simpler method is to use a device dubbed the "Autotrak". This device, which is more fully discussed in the section on timing, automatically maximizes the beam intensity for any given injection energy by means of a feedback system which regulates injection timing.

The average operating lifetime of an injector is about 60 to 70 hours

when the filament current is maintained in the recommended range of 6 to 7 amps. The average lifetime decreases when the injectors are run at higher voltages and higher filament currents. With lower filament current and injection voltages below 90 kv, some injectors have lasted well over 200 operating hours; the record was 327 hours. The usual cause of injector failure is filament evaporation, which can cause open filament or high filament resistance and low beam intensity.

E. Timing

The times during the magnet cycle at which various events happen --injector fires, resonator starts, resonator stops--must be closely timed if successive bursts of electrons are to be uniform in energy and intensity. A variation of 0.1 μsec in the time at which the injector fires, for example, can cause the gamma-ray output from the target to vary by a factor of two.

All timing is referred to a signal received from a peaking strip placed in the magnet gap. The peaking strip consists of a thin ribbon of high-permeability alloy placed vertically in the magnet gap and wound with a coil of about 100 turns. As the magnetic field passes through zero, the flux in the strip goes very rapidly from saturation in one direction to saturation in the other direction, inducing a sharp voltage pulse in the coil. This pulse is differentiated for increased sharpness and amplified. Before the peaking-strip signal is allowed to trigger any timing devices, a gate eliminates those pulses which arise when the magnetic flux in the gap is decreasing through zero and passes only those pulses which arise when the flux is increasing through zero in the proper direction. The gating device is a pentode in which the peaking signal goes to the grid and the voltage from a wire loop around the flux bars goes to the screen; the polarity of the screen is selected to make the tube conducting for the proper flux condition.

A block diagram of the timing circuit is shown in Fig. 18. The pulse
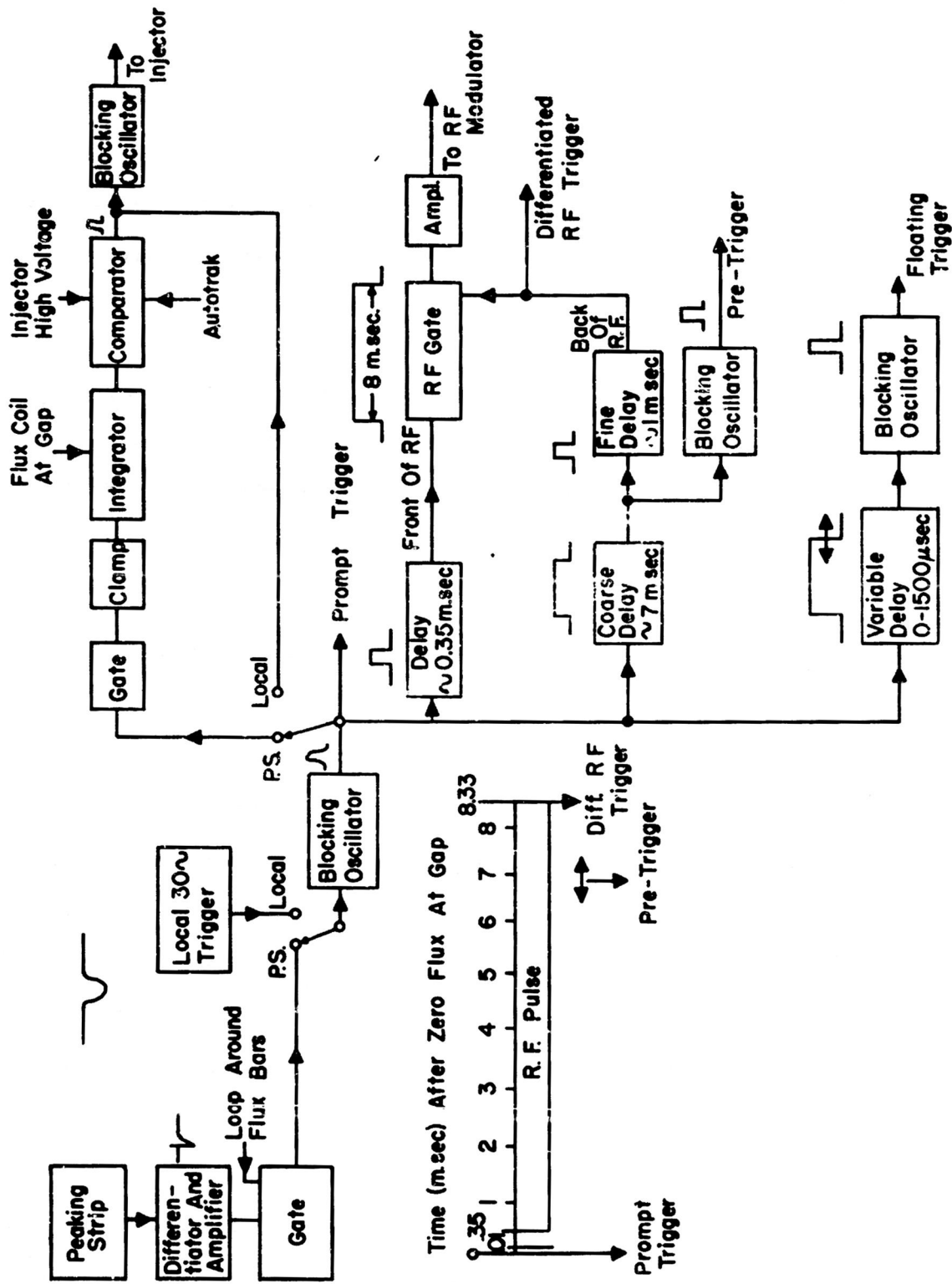
Fig. 18 Block Diagram Timing Circuit

from the peaking strip, by opening a grounding clamp, starts an integrator in
the part of the circuit which fires the injector. The integrator provides a
comparator with a potential proportional to the flux density in the magnet gap.
This potential and the high voltage from the injector firing circuit are compared
in a 2-triode univibrator whose output pulse triggers the thyratron in the
injector firing circuit. By adjusting the grid bias on one of the triodes, the
injector can be made to fire at the optimum time for a given value of injector
high voltage. Once the bias is set, the comparator will continue to fire the
injector at the same value of gap flux density on succeeding cycles, despite
small fluctuations in magnet excitation of injector high voltage.

In testing the timing circuit when the magnet is not being energized,
a local 30-cycle trigger circuit is substituted for the peaking-strip signal;
this local signal goes directly to the blocking oscillator which feeds the in-
jector trigger because the integrator, and hence the comparator, is inoperative
when the magnet is not being operated.

The delays which time the input to the modulator in the radiofrequency
circuit are set to start the modulator when the electrons have reached the
energy of transition from betatron to synchronous acceleration and to stop the
modulator when the electrons have reached some predetermined energy. For maximum
electron energy, the modulator is activated until the flux in the magnet gap is
at its peak. The electron energy at the target may be reduced either by shorten-
ing the period of activation of the radiofrequency modulator, or by decreasing
the magnet current; the latter method has proved preferable when a gamma-ray
beam of long duration is desired, but both methods are used.

The timing circuit also provides two extra trigger pulses which were
included in anticipation of experiments in which the timing of the detector would
be tied in with the time of the beam pulse. The "pre-trigger" signal can be made
to precede the end of acceleration by a short, variable time, while the "floating
trigger" can be adjusted to give a signal which follows the peaking-strip signal

60

by any fixed interval from zero to 15,000 μsec. The "floating trigger" has been
used extensively. The "prompt trigger" and "differentiated RF trigger" have been
used mainly as oscilloscope sweep triggers for adjusting the timing circuit and
for observing the output of various beam detectors.

A feedback device called the "Autotrak" can be used in connection with
the injector trigger circuit to maximize the electron beam intensity for any given
injection energy. The Autotrak output is used to bias the comparator, thus vary-
ing the time at which the injector fires. The input to the Autotrak is a 30-cycle
signal from a photomultiplier tube which is activated by light radiated by the
electron beam (see the section on synchrotron operation for details on the "light-
meter"); the magnitude of the photomultiplier pulse varies with the beam intensity.
In the Autotrak, a crystal diode bridge circuit between the input and a scale-of-
two inverts the sign of every second pulse from the photomultiplier. The resultant
alternating signal is fed to an integrator, which, in turn, sends a signal to a
"wiggler" component. The wiggler provides instability in the injector timing by
alternately increasing and decreasing the comparator bias by small amounts on
successive pulses. A signal from the integrator causes the wiggler to "track",
that is, to increase or decrease the average comparator bias. The direction in
which the timing changes depends upon the sign of the integrator signal, which in
turn depends upon the relative beam intensities produced by the higher and lower
signals from the wiggler. The circuit is designed to track toward higher intensity.
When maximum intensity is reached, the integrated signal will be zero and the
wiggler will stop tracking; it will resume tracking if the beam intensity on
alternate pulses is not the same.

F. Circuits and Wiring

The control circuits, in general, were built to follow the system developed at the University of California Radiation Laboratory at Berkeley. All components of the synchrotron can be operated from a central control desk, or console, located some 60 ft. from the magnet and shielded by about 30 ft. of earth and concrete. Duplicate controls are located near the machine for checking particular components. All relays, switches, interlocks, etc., are wired directly to a central cross-connect panel, and the circuits are hooked up by point-to-point wiring on this panel. Control and power wiring are kept separate. Remote control has been used wherever possible in order to keep power wiring out of the control room.

III. OPERATION OF THE SYNCHROTRON

A. Calibration

Before the synchrotron becomes a useful tool, its output must be calibrated. The calibration includes measurements of the following quantities:

1. The energy of the electrons at the time they strike the target

2. The time distribution of the beam pulse

3. The gamma ray spectrum

4. The total gamma ray intensity

5. The angular distribution of the gamma rays

This section is devoted to a discussion of what has been learned about these quantities.

1. Electron energy

The energy of the electrons striking the target has been determined by measuring the magnetic field of the synchrotron and also by measuring the endpoint of the gamma ray spectrum. The field was explored with a rotating coil, which had been calibrated against a flux meter using the proton magnetic moment as a standard. The spectrum measurements were made with the magnetic pair spectrometer which was calibrated absolutely by a current-carrying wire. Both measurements agreed to within one percent and gave an electron energy of 315 Mev at the peak of the cycle under standard operating conditions. These measurements were carried out during 1951. In December 1952 the 3 1/4 inch gap in the synchrotron magnet was increased by 1/16 inch, thus lowering the electron energy to 309 Mev.

2. Beam pulse time distribution

For most experiments it is desirable to spread the beam pulse in time in order to reduce accidental coincidences in the counting equipment. This is accomplished by shaping the envelope of the signal on the RF cavity in such a way

that the RF voltage slowly decreases below what is required to maintain phase stability. Generally the beam pulse is spread to 2-3 milliseconds. Under these conditions the electrons striking the target vary in energy and have an average energy less than the peak reading. For a typical beam pulse of width 2.5 milliseconds the average energy is reduced by about 6 Mev at the peak of the cycle. The time distribution is observed directly with a scintillation counter whose output is displayed on a linear sweep. The energy effect of the time spread has been observed by the spectrometer in measurements described below.

3. The gamma ray spectrum

For an ideal thin target the shape of the gamma ray spectrum will be the so-called bremsstrahlung spectrum. A target having a thickness of about one-tenth radiation length or more would be expected to show a spectrum measurably altered by electron energy loss, multiple events, and gamma ray absorption. Even a thin target spectrum is difficult to predict due to the phenomenon of multiple traversals, demonstrated by Camac[24]. The problem is further complicated by the possibility that the spectrum in the core of the beam may be different from that at the edge.

Measurements on the spectrum have been made by DeWire and Beach[25] using a magnetic pair spectrometer. The spectra for thin (1/2 mil W ribbon) and thick (40 mil W wire) targets are shown in Figs. 19 and 20. There appears to be a somewhat larger portion of soft quanta relative to hard for the thick target compared to the thin target, the magnitude of this effect being about five percent. Other runs have been taken with closer spacing of points near the upper energy limit. These data show good agreement between thick and thin target and indicated that the electron energy loss in the target is certainly less than ten percent. The effect of the time spread of the beam has also been observed and gives reasonable agreement with the predicted energy spread.
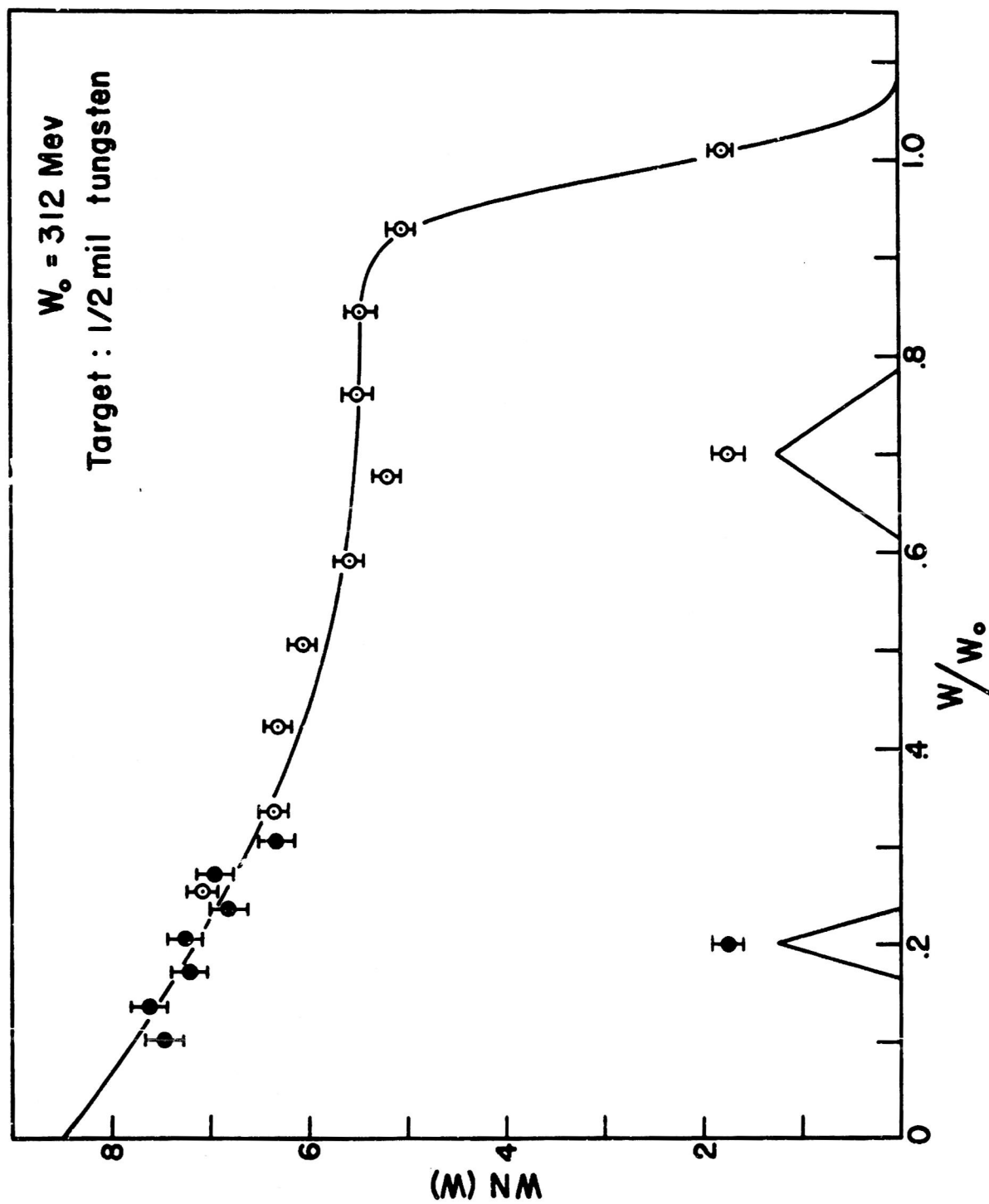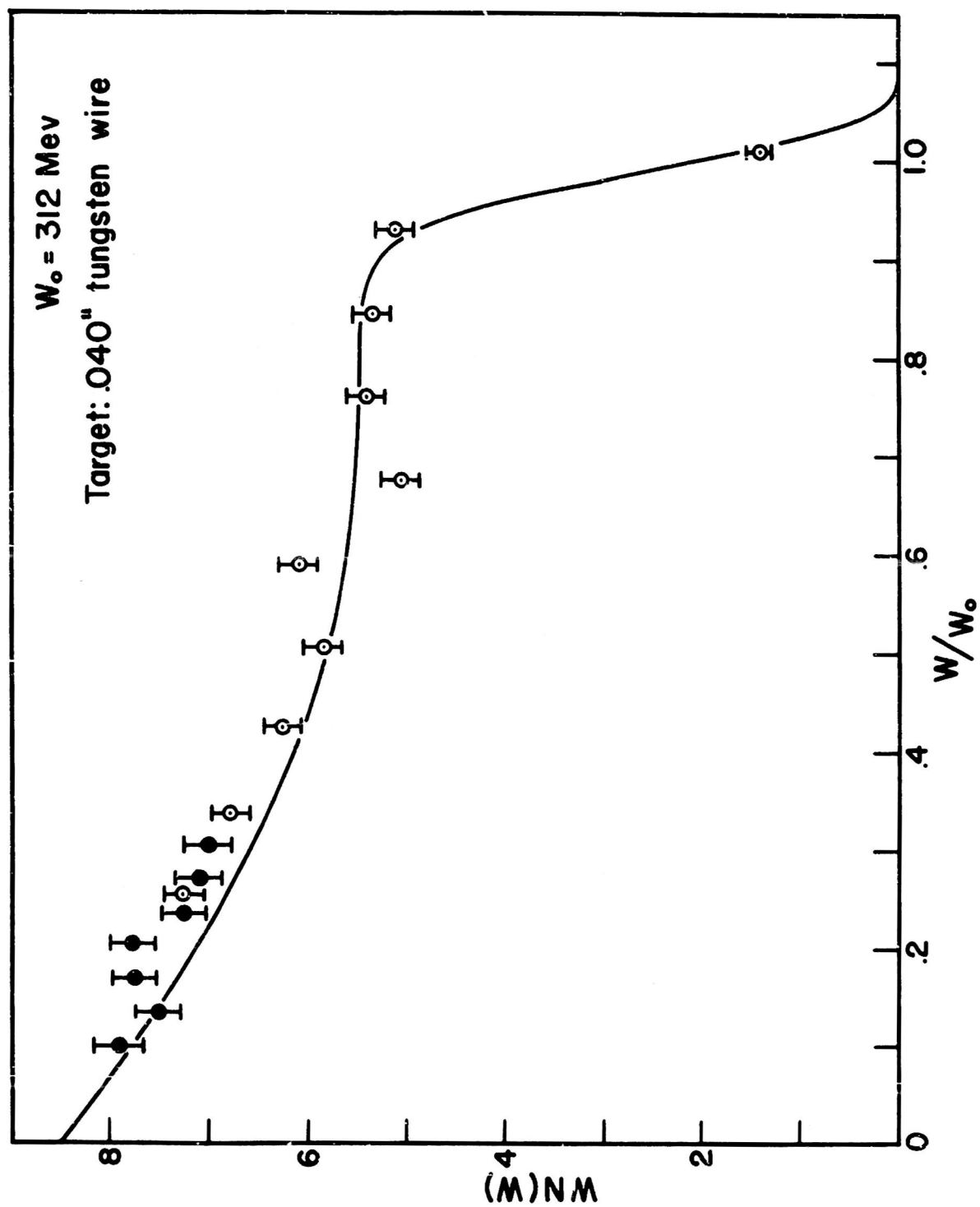
Fig.19 Thin Target Spectrum

W_o = 312 Mev
Target: .040" tungsten wire

W/W$_o$

WN(W)

Fig. 20 Thick Target Spectrum

The accuracy of these measurements is limited by the ten percent energy resolution of the spectrometer. The shape of the resolution function is rather well known but its presence materially reduces the steepness of the spectrum cut-off.

The spectrometer results are believed to give the relative spectral shape to five percent in the region from one-tenth to nine-tenths the maximum energy W_o and to twenty percent in the region 0.90 W_o to 0.95 W_o.

4. The total gamma ray intensity

The total gamma ray intensity from the synchrotron is normally specified in "equivalent quanta" or Q which are defined as the total energy of photons U divided by the maximum photon energy W_o, i.e.

$$Q = U/W_o = 1/W_o \int_0^{W_o} W \, n(W) \, dW$$

where W is the photon energy and $n(W)dW$ is the number of photons between W and $W + dW$. A rough approximation to the bremsstrahlung spectrum is $n(W) = k/W$, in which case $Q = k$. In any case a specification of Q and of the spectral shape allows a determination of $n(W)$.

The standard instrument for measuring the beam intensity is the ionization chamber shown in Fig. 21. The chamber walls are of such a thickness that the charge developed is largely due to ionization by electrons of a shower near the shower maximum. Since the number of electrons at the shower maximum per incident photon is roughly proportional to the photon energy, the charge collected on the chamber electrodes will be roughly proportional to the total energy in the beam U. For this reason the sensitivity of the chamber is most reasonably expressed in units of Mev/coulomb.

The charge collected in the chamber is measured by a vacuum-tube electrometer designed by Littauer[26]. The effect of ion recombination has been
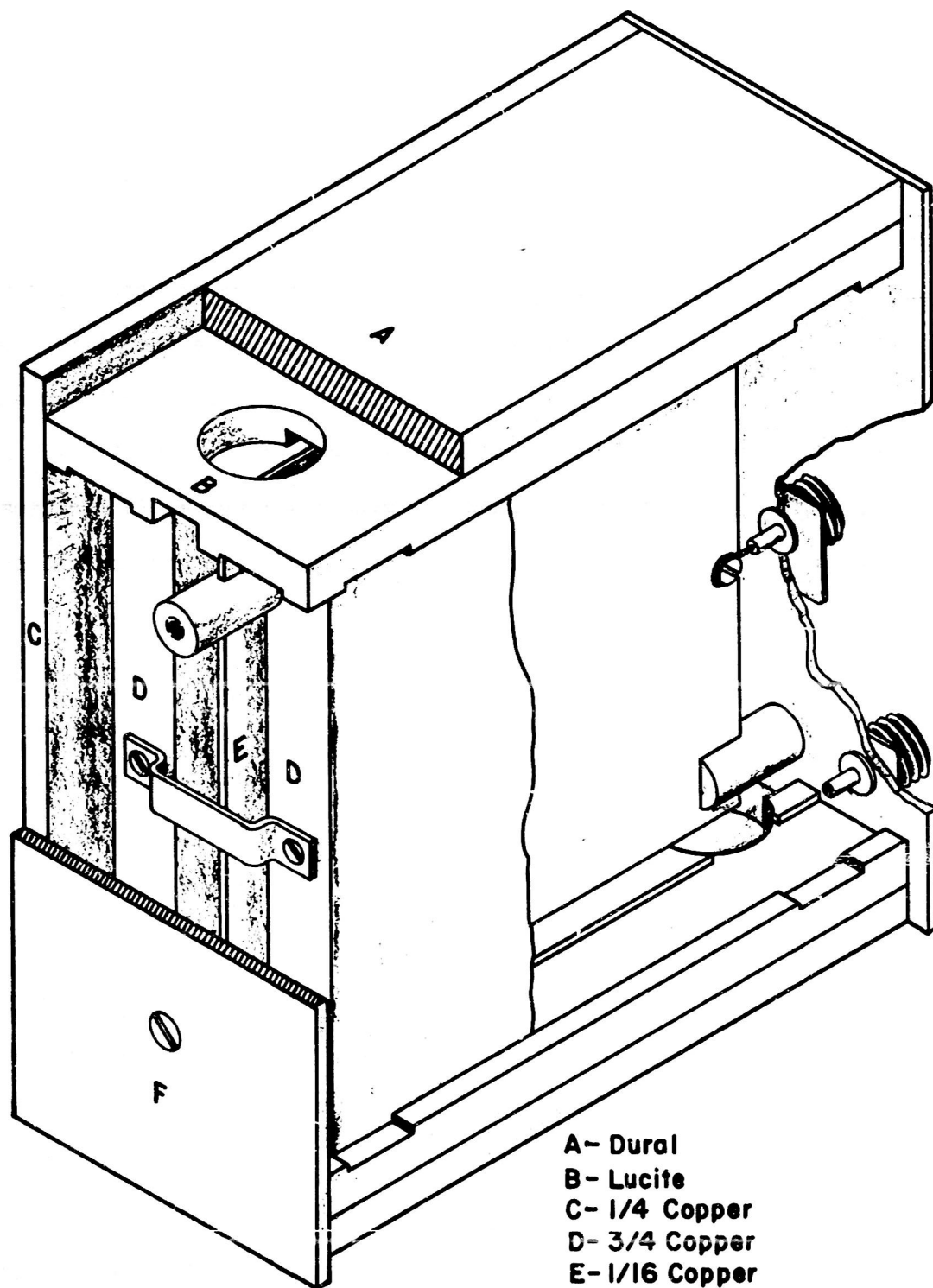
A— Dural
B— Lucite
C— 1/4 Copper
D— 3/4 Copper
E— 1/16 Copper
F— Dural

Fig.21 Standard Ionization Chamber

studied. The result can be expressed by the relation

$$I/I_0 = e^{-V_0/V}$$

where I = observed ion current, I_0 = saturation ion current, V = voltage applied to chamber, and V_0 is a constant proportional to the incident radiation density (per unit area) and to the square of the depth of the ion chamber. The pulse length does not affect this relation so long as the ion collection time, about 10^{-2} sec, is long compared to the pulse time. In a typical experimental arrangement, we have measured $V_0 \approx 7$ volts for our standard copper ion chamber, at a beam intensity of 4×10^9 equivalent quanta per minute through a 3/4" collimator. Since the chamber is normally operated at 350 volts, the recombination loss at this beam intensity would be of the order of 2%.

The chamber has been calibrated in two ways: (1) against the pair spectrometer and (2) by the shower method developed at California[27].

The comparison with the spectrometer was done by allowing a collimated beam to pass through the spectrometer to strike the face of the standard chamber. The collimating slit was 3/8" x 1" and was approximately 11 meters from the synchrotron target, so that only the central portion of the beam was used. The number of quanta was determined from the counted pairs, the known radiator thickness, the calculated geometrical efficiency of the spectrometer, and the pair cross section which can be obtained from data on the absorption of high energy gamma rays. Runs were made with thin Al and Cu radiators and with several ionization chambers which were then intercalibrated. For the standard chamber the sensitivity was found to be 3.74×10^{18} Mev/coulomb at NTP. This figure is believed to be accurate to 5%.

The shower method was used to obtain an independent check on the absolute calibration and also to measure the dependence of the sensitivity on the energy setting of the synchrotron. The shower curve was measured in a stack of aluminum slabs two inches thick and twelve inches square. The ionization was determined

by inserting a thin chamber between slabs. A typical curve is shown in Fig. 22.

This method does not yield an absolute calibration, because the density effect on the energy loss in aluminum relative to air is not known precisely. A maximum error of 5% has been estimated for this effect. Sensitivities obtained from these measurements, uncorrected for the density effect, are 3.74 Mev/c at 315 Mev, 3.59 Mev/c at 250 Mev, and 3.47 Mev/c at 197 Mev.

Our best beam intensity has been about $3x10^{10}$ equivalent quanta per minute. More typical values under good operating conditions range about $5x10^9$ equivalent quanta per minute.

The magnitude of the circulating electron current in the synchrotron is monitored by measuring the amount of light radiated by the continuously accelerated electrons. The light is brought to a photomultiplier tube by a mirror and lucite light pipe. The output of the tube is fed to the circuit shown in Fig. 23 which gives a logarithmic response and is used to operate large meters in the accelerator room as well as a pen recorder in the control room.

5. The angular distribution of the gamma rays

It is sometimes important to know the angular distribution of the gamma rays to evaluate the results of experiments where the beam intensity varies appreciably over the face of the irradiated target. An approximate formula for the angular distribution taking into account the angles of emission of the quanta and the multiple scattering of electrons in the target has been derived by Schiff[28].

Measurements on the angular distribution have been made by Luckey in this laboratory. The method involved making exposures of known relative intensities of standard X-ray film behind 1/16 inch lead. Then regions of equal blackening were plotted for the different exposures. A curve giving relative intensity per unit area as a function of angle is given in Fig. 24.

Fig 22 Typical Shower Curve In Al
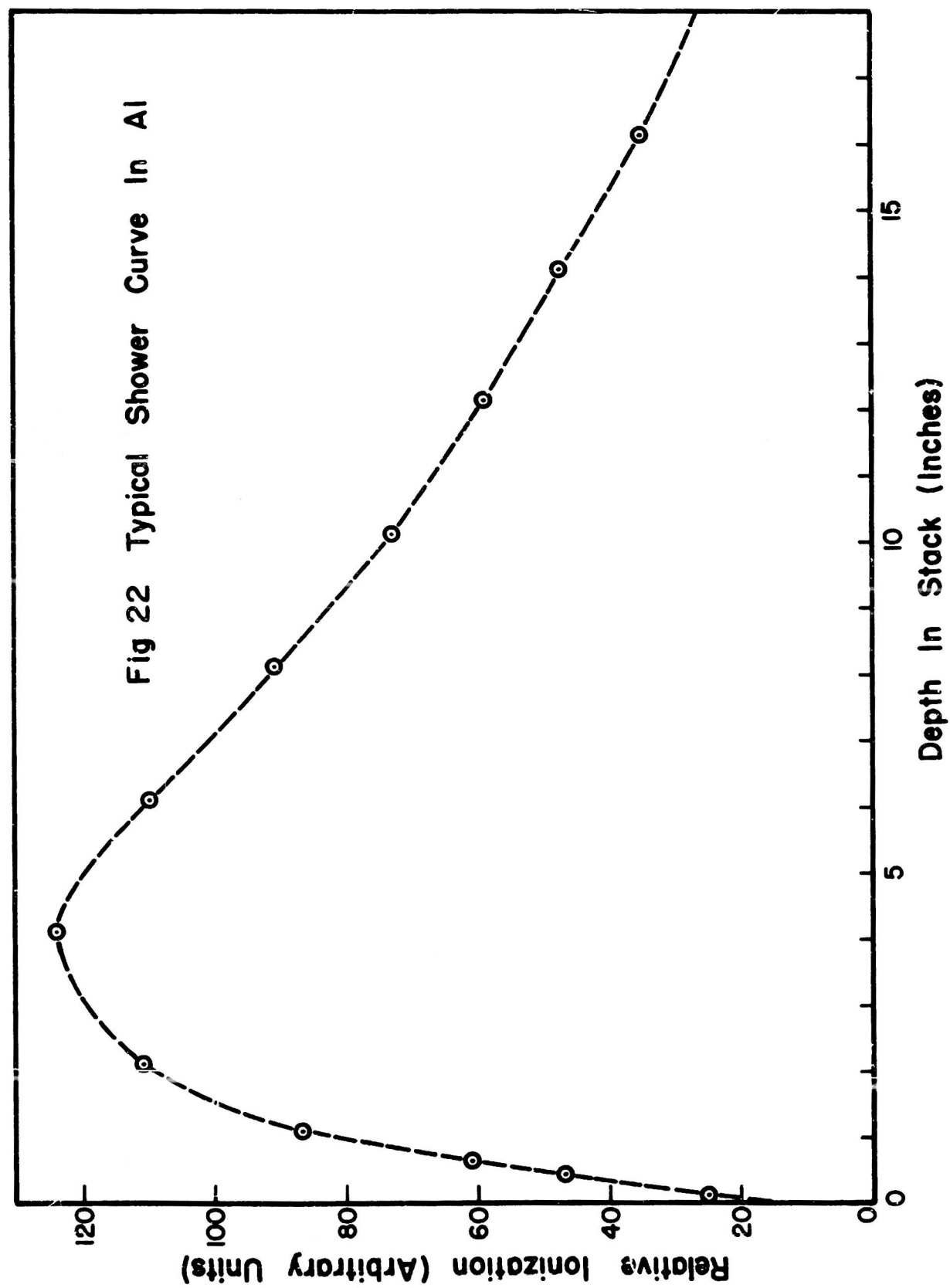
Comparison with Schiff's formula gives an effective target thickness of 0.05 radiation length. It should be pointed out that this method measures the angular distribution of soft quanta, so that the effective target thickness may be somewhat smaller than that quoted.

B. Radiation Shielding

By piling large concrete blocks as indicated in Fig. 25 it has been possible to keep radiation levels low enough to permit experimenters to work within reasonable distances of the synchrotron. At beam levels of 10^{10} Q/min, however, the fast neutron levels in the synchrotron room become uncomfortably high for protracted exposure. Consequently all our detecting equipment has been moved to a detector room, separated from the synchrotron room by a minimum of 30 feet of earth.

Fig. 25 gives measured radiation levels at various points in the room. Gamma ray levels are given in milli-R per hour and are measured with commercial ionization chamber type radiation meters. Fast neutron fluxes are given in neutrons/cm^2/sec and have been measured with silver foils immersed in water and with BF_3 counters buried in paraffin. These radiation levels are referred to a beam intensity of 10^{10} Q/min as recorded behind a $\frac{1}{2}$ inch x $\frac{1}{2}$ inch collimator located approximately two meters from the synchrotron target.
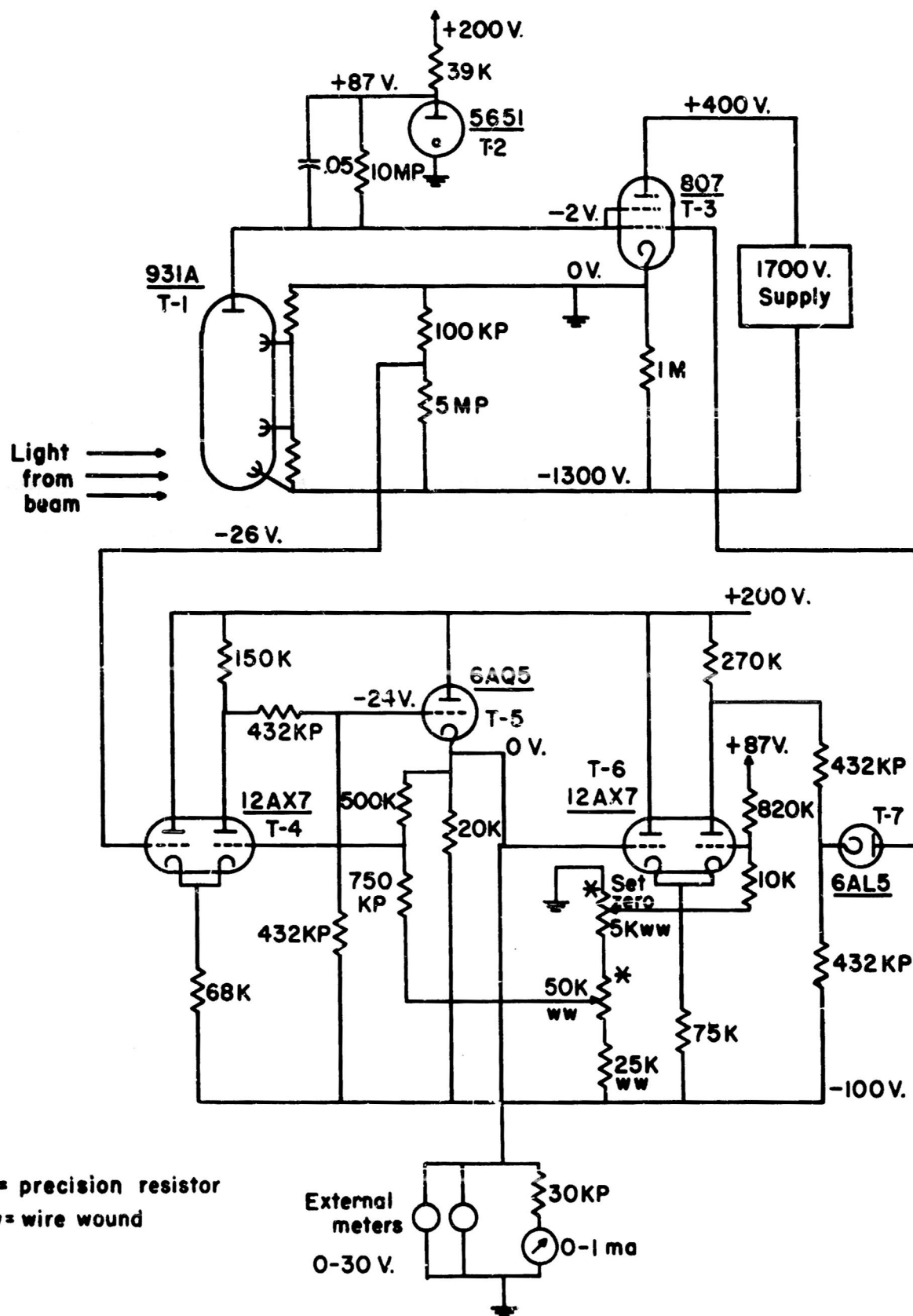
Fig. 23 Light Meter

Fig. 23. Light Meter Circuit

The light meter monitors the synchrotron beam by measuring the visible light radiated by the electrons as a result of their centripetal acceleration. This light is reflected out of the donut by a system of mirrors, and allowed to fall on the cathode of a photomultiplier. The external circuit is arranged to turn down the voltage applied to the phototube until the current out of the tube is reduced essentially to its zero-beam value. The amount by which the voltage must be reduced is a convenient, non-linear measure of the beam intensity.

The circuit is very simple. In the absence of any light a steady dark-current of 9 μa. flows in the phototube T-1. The current is supplied from the VR tube T-2 through a precision resistor. The normal voltage applied to the phototube is about 1300 v., but when light from the beam causes the current from T-1 to increase it drives the grid of T-3 negative, causing this tube to absorb a greater fraction of the total voltage from the power supply (1700 v.). Thus, the net voltage applied to T-1 is decreased, and at equilibrium the output current of the tube is again close to 9μa. The time-constant is made long compared to 1/30 sec. to integrate over several beam-pulses. The individual pulses vary in height as the beam does, although their average magnitude is held constant, and can be used for automatic tracking of the injection-time.

1/50 of the photomultiplier voltage is tapped off by a resistance divider, and fed to the first grid of T-4. T-4 and T-5 together form a feed-back differential DC amplifier of low gain. The 24 v. bias on T-5 brings the signal to ground potential in the absence of any light falling on the photo-tube, and the cathode of T-5 gives a positive-going signal at low impedance when radiation from the beam brings the circuit into operation. Any number of 30 v. voltmeters can then be used externally as indicators.

T-6 and T-7 are inserted to stabilize the zero-point. As the photo-current injected into the circuit is reduced, the grid of T-2 rises in potential until the diode T-7 begins to conduct. The circuit then forms a closed loop inversely fed-back, and clamps at the proper zero-level. The reference-voltage for T-6 is used as a zero-set. In practice it has been found that no adjustment is necessary over periods of several weeks.

Fig.24 Angular
Distribution of Gamma
Rays
312 Mev
0.040" W. Target
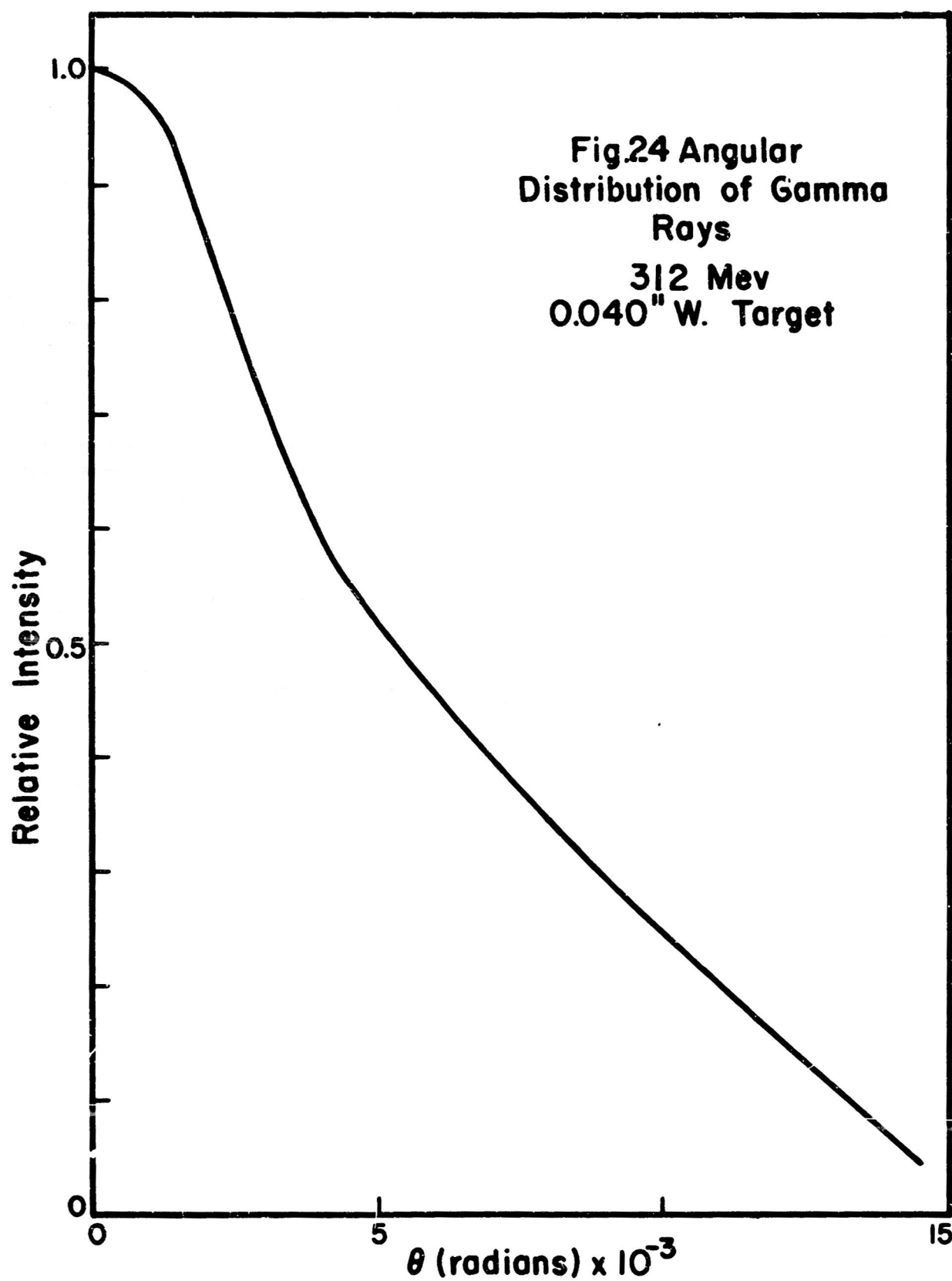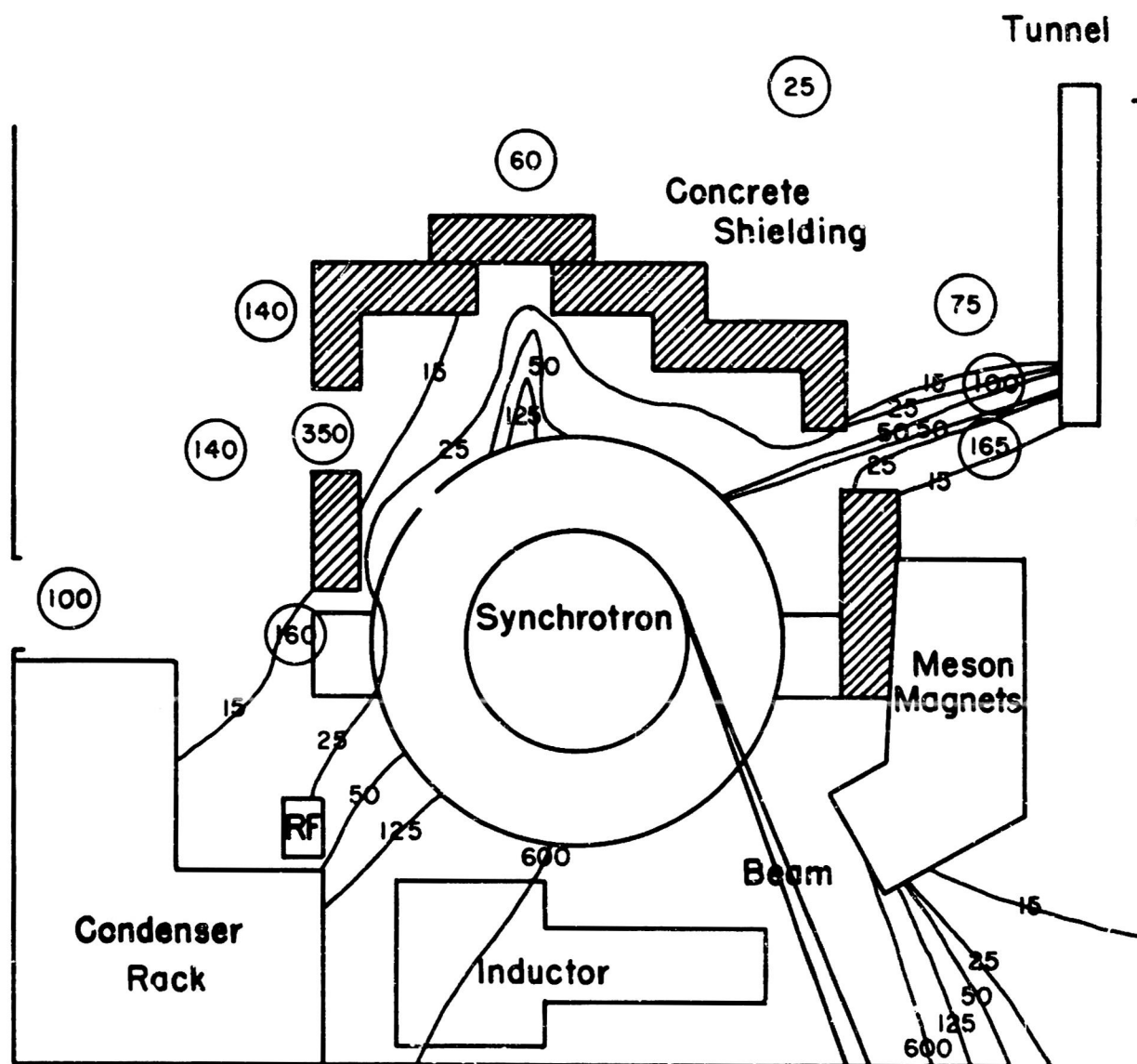
Beam Intensity = 10^{10} Q / Min.

25 Fast Neutron / cm^2 / sec

600 Gamma Ray dosage rate in mr/hr

Fig.25 Radiation Level around Synchrotron

76

IV.   IV.   ACKNOWLEDGMENTS

The synchrotron in its completed form represents a great amount of work by many people. We want particularly to thank our colleague, Professor W. M. Woodward, who engineered the radiofrequency system in its present reliable form. Many of the electronic refinements are the work of Dr. R. M. Littauer. Our machine shop, under the supervision of Mr. C. F. Van Amber, has undertaken the most difficult jobs with enthusiasm and completed them with dispatch. We want to thank the many graduate students whose devoted service has been vital at every state of construction and operation of the machine.

It is evident that the whole project would have been impossible without the generous support of the Office of Naval Research.

REFERENCES

1. E. M. McMillan, Phys. Rev. 68, 143 (1945).

2. V. Veksler, J. Phys. U.S.S.R. 9, 153 (1945).

3. J. H. Fremlin and J. S. Goodin, Reports on Prog. in Phys. 13, 331 (1950).

4. Wheeling, West Virginia.

5. Camden, New Jersey.

6. General Electric Company, Schenectady, New York.

7. Brooklyn, New York.

8. Armco Steel Corporation, Middletown, Ohio.

9. Chicago, Illinois.

10. General Electric Company, Schenectady, New York.

11. E. D. Courant, Rev. Sci. Instr. 20, 611 (1949).

12. D. Bohm and L. Foldy, Phys. Rev. 70, 249 (1946).

13. Corning Glass Works, Corning, New York.

14. Bakelite Company (Division of Union Carbide and Carbon Corp.), New York, N.Y.

15. General Electric Company, Schenectady, New York.

16. Kinney Manufacturing Company, Boston, Massachusetts.

17. Distillation Products Incorporated, Rochester, New York.

18. Radio Corporation of America, Harrison, New Jersey.

19. C. S. Nunan, Thesis for M.S. Degree in Electrical Engineering, University of California, 1940.

20. Corning Glass Works, Corning, New York.

21. Amersil Corporation, Hillside, New Jersey.

22. Insl-X Company, Ossining, New York.

23. New England Transformer Company, Somerville, Massachusetts.

24. Morton Camac, Rev. Sci. Instr. 24, 290 (1953).

25. J. W. DeWire and L. A. Beach, Phys. Rev. 83, 476 (1951).

26. R. M. Littauer, Rev. Sci. Instr. (in press).

27. Blocker, Kenney, and Panofsky, Phys. Rev. 79, 419 (1950).

28. L. Schiff, Phys. Rev. 70, 87 (1946).